FACULTY OF TECHNOLOGY

CONCEPT MODELING OF ENERGY EFFICIENCY FOR HEAVY-DUTY TRUCKS WITH E-AXLE EQUIPPED TRAILER

Jaakko Kinnunen

DEGREE PROGRAMME IN MECHANICAL ENGINEERING

Master's Thesis

July 2023

ABSTRACT

Concept Modeling of Energy Efficiency for Heavy-Duty Trucks with E-axle Equipped Trailer

Jaakko Kinnunen

University of Oulu, Degree Programme in Mechanical Engineering

Master's thesis 2023, 97 pp.

Supervisor(s) at the university: Juho Könnö, Perttu Niskanen

The purpose of this master's thesis is to study potential of E-axle on a trailer to provide better maneuverability for heavy trucks, and the possibility of fuel savings and thus lower tailpipe emissions and operating costs of the vehicle. Three different truck combination types were studied, timber, tipper, and long-haul trucks. Real-life driving data and other information of the selected truck types are collected, and simulation model of the trucks are created with MATLAB. Models are validated by comparing the simulation results with the collected real life driving data. After validation, E-axle is added to the model and the potential of the E-axle is tested in the abovementioned use cases. The results indicate that even a relatively small battery of 20 kWh could yield substantial fuel savings in the range of 5 – 15 %, depending on the drive cycle. If battery has to be charged by driving operations, the net fuel saving ranges between -1–9 %. However, the used control logic for the E-axle in this study was very simple and better overall results can be expected with optimized system. Substantially increased hill climbing ability in highway speeds with E-axle was also demonstrated, even with downgraded engines. Findings provide good general information about the potential of E-axle in timber, tipper, and long-haul trucks.

Keywords: truck, E-axle, electric, hybrid, simulation

TIIVISTELMÄ

E-akselilla varustettujen raskaiden kuorma-autojen energiatehokkuuden konseptimallinnus

Jaakko Kinnunen

Oulun yliopisto, Konetekniikan tutkinto-ohjelma

Diplomityö 2023, 97 s.

Työn ohjaaja(t) yliopistolla: Juho Könnö, Perttu Niskanen

Tämän diplomityön tarkoituksena on tutkia peräkärryyn asennettavan sähköisen akselin, eli E-akselin hyödyntämistä raskaiden ajoneuvojen liikkuvuuden parantamisessa, sekä kulutuksen ja siten päästöjen ja käyttökulujen pienentämisessä. Työn kohteena on kolme erilaista raskasta ajoneuvoyhdistelmää, puuauto, sora-auto, sekä kaukoliikenneauto, joista kerätään ajomittausdataa reaaliympäristössä. Kirjallisuudesta ja tutkimuksista hankittujen ajoneuvon tietojen, sekä kerätyn ajodatan perusteella luodaan ajoneuvoista simulointimallit MATLAB-ohjelmistolla, jossa mallin toimivuus validoidaan vertaamalla simuloinnissa saatuja tuloksia mitattuihin tuloksiin. Kun mallin toimivuus on varmistettu, lisätään malliin E-akseli ja verrataan ja arvioidaan E-akseli potentiaalia yllä mainituissa tapauksissa suhteessa tavalliseen autoon. Tulokset antavat olettaa, että jo suhteellisen pienellä akkukoolla kuten 20 kWh, voi olla mahdollista saavuttaa ajosyklistä riippuen 5–15 % polttoainesäästöjä. Mikäli akku joudutaan kuitenkin lataamaan ajamalla täyteen, niin nettopotentiaali voi vaihdella -1–9 % välillä. Täytyy kuitenkin muistaa, että tässä työssä käytetty ohjauslogiikka E-akselille on hyvin yksinkertainen ja siten voidaankin olettaa, että kunnollisella optimoidulla ohjauslogiikalla on mahdollista saavuttaa yleisesti ottaen parempia tuloksia. Myös mäennousukyvyssä huomattiin huomattava parannus E-akselilla varustetuissa ajoneuvoissa, myös tapauksissa, joissa moottorin kokoa oli pienennetty alkuperäisestä. Tulokset antavat yleispätevää tietoa E-akselin potentiaalista puuautossa, sora-autossa ja kaukoliikenne käytössä.

Asiasanat: kuorma-auto, e-akseli, sähkö, hybridi, simulointi

PREFACE

This Master's thesis was done as part of Business Finland project in collaboration between University of Oulu and VTT Oy, as part of a project to develop energy efficiency of vehicles and competence in this field in Finland. The project started in January 2023 and continues on.

I would like to thank Research Team Leader Petri Söderena for providing me with this thesis opportunity. I would also like to thank my supervisors Prof. Juho Könnö and Lect. Perttu Niskanen at the University of Oulu for their guidance in this work, as well as Senior Scientists Pekka Rahkola and Shah Sahas for giving guidance as well. I would also like to thank all the colleagues at VTT who have helped and contributed to this project. Also Special thanks to Korsu Oy, Kuljetusliike Eskola Oy and Maanrakennus A. Sappinen Ky for their contribution to this work.

Oulu, 5.7.2023

Jaakko Kinnunen

TABLE OF CONTENT

LIST OF SYMBOLS AND ABBREVIATIONS

A	surface area
B	fuel consumption
b_e	break specific fuel consumption
c_w	air drag coefficient
F_L	aerodynamic resistance
f_R	rolling resistance coefficient
F_{ro}	rolling resistance
F_{st}	climbing resistance
F_w	total running resistance
g	gravitational acceleration
H_u	fuel specific calorific value
I	current
i	ratio
kW	kilowatt
m	mass
M	torque
n	rotational speed
P	power
P_w	total running power
r	radius
U	voltage
v	vehicle speed
W	watt
α	angle
η	efficiency
η_e	engine efficiency
π	pi
ρ	air density
Ω	resistance

BEV	Battery Electric Vehicle
BSFC	Brake Specific Fuel Consumption
CAN	Controller Area Network
EM	Electric Machine
EV	Electric Vehicle
GCL	Gearbox Control Logic
HDV	Heavy Duty Vehicle
ICE	Internal Combustion Engine
LFP	Lithium Iron Phosphate
MCL	Motor Control Logic
NMC	Nickel Manganese Cobalt
PI	Proportional-Integral
SOC	State of Charge
WLTP	Worldwide Harmonized Light Duty Vehicle Test Procedure
ZEV	Zero-Emission Vehicle

1 INTRODUCTION

Powertrain electrification has taken significant steps in the passenger car industry but is lacking behind in heavy-duty vehicles (HDV), while at the same time the green transition is an ongoing phenomenon that every industry must react to and do their best to lower the emissions. According to EU's latest proposal 2023/0042COD, heavy duty vehicles (HDV) in Europe account for over 6 % of the total EU greenhouse gas emissions and aim is to reduce emissions by 65 % by the year of 2035 compared to 2019 levels. However, this proposal is not active yet, but still gives an idea of the future for all vehicles.

Full electrification of the truck powertrain; however, is not a solution to all the problems, since battery packs are expensive and heavy, thus decreasing the overall capacity/efficiency of the truck, depending on the intended usage. Also, material availability for electric motors and batteries can also be considerable problems, as well as the possible dependency on handful of suppliers for these materials. (IEA 2022, pp.154–156) At the time of writing this master's thesis, there were new propositions from EU for the definition of a "zero-emission-vehicle" (ZEV) such that ZEV can mean following vehicle: *"a trailer equipped with a device that actively supports its propulsion and has no internal combustion engine or has an internal combustion engine emitting less than 5 g CO2/kWh as determined in accordance with Regulation (EC) No 595/2009 of the European Parliament and of the Council and its implementing measures or UNECE Regulation (EC) No 49."* (EU COM/2023/88 final, p.21) In this master's thesis, the potential of electrified trailer axle, more commonly known as E-axle is studied on three different HDV applications: timber truck, tipper truck and long-haul truck. The different study cases for these applications are:

- potential for improved fuel consumption with only the E-axle added, and with E-axle and downgraded engine power.
- potential for improved traction force especially for timber and tipper trucks.
- potential for running auxiliaries with electricity provided by the traction battery of the E-axle system.

Currently there are no E-axle solution available for timber or tipper trucks, and especially in the form of Nordic countries trailer type. However, the idea of driven axle on trailer is not a new idea. Already back in the 60s, Sisu developed fluid motor driven axle called Nemo (Nestemoottori) which was greatly praised for its traction capabilities. Vehicle combination of those days had theoretical climbing ability of 25 % hill grade with friction coefficient of 0,4. (Mäkipirtti 2011, p.178)

In this study, it is expected that a trailer with an E-axle can provide better energy efficiency of the vehicle by restoring otherwise lost energy in decelerations of the vehicle or by charging the battery from mains electricity and also to provide better traction for difficult road conditions. It is also expected that an E-axle can offer fuel savings in up hills due to increased overall performance of the vehicle. The problem is studied by creating a simulation model of the above-mentioned truck combination types in which both conventional drivetrain is evaluated based on real-life driving data as well as hybrid E-axle drivetrain is evaluated by comparing its performance against the conventional powertrain in areas of fuel consumption (energy efficiency) and mobility.

1.1 Overall Characteristics of the Vehicles and E-axle Potential

The vehicles considered in this study are European N3-class vehicles, meaning commercial vehicles with total mass over 12 000 kg. In Finland the total vehicle combination mass is 76 tons if the combination has at least 11 axles, or 9 axles if at least 65% of the mass of the trailer or of the total mass of the trailers is applied to axles fitted with twin wheels. (Tieliikennelaki, 122 §, appendix 6.6) Timber truck combinations today typically have 4 axles with 5 axle trailer and same can apply to tipper truck combinations as well. The addition of an E-axle will practically convert a conventional truck combination into a hybrid vehicle, and more specifically into a parallel-axle-hybrid vehicle.

The driving characteristics of a timber truck consists of tarmac roads as well as narrow and small forestry roads with possibly high hills without the possibility to gain high speeds to climb them up. Also, significant portion of the work is done during winter when roads are icy and slippery, so that use of traction chains can be often needed. In such

conditions the E-axle on the trailer could potentially provide additional traction power to move the vehicle up the hill and possibly the need for using traction chains could decrease, thus time and effort could be saved for not needing to stop for installing or taking them off. Other key characteristic of timber truck is that it will usually drive empty to some direction since forestry locations are located far from the trucking company's base and location where load should be delivered is typically quite far from the pickup point as well. With the E-axle some of the energy otherwise lost in downhill coasting or in braking can be recuperated back into the system to help propel the vehicle or possibly, in theory, support crane operations. It might also be possible to load the trailer first in conditions where you would normally not do that, since the trailer can assist in the movement of the vehicle.

In tipper truck operations the benefits of E-axle are mostly same as for timber truck; improved traction in difficult road conditions or otherwise improved climbing ability of the combination. Auxiliaries could similarly be powered by the regenerated energy, for example tipping of the bucket. Technically, it may also be possible to recuperate energy from the downward movement of the bucket against gravity to generate electricity, similar to what some excavators have for boom movement recuperation. However, same thing can be achieved with hydraulic recuperation.

For long-haul truck it can be considered that they are driven mostly full, and thus the most interest in the E-axle comes from the possibility to downsize the engine to make it operate more efficiently. In plain tarmac road conditions, the energy need to move the vehicle is small, compared to accelerating the vehicle from the standstill or when climbing up hills. This is where the E-axle could help and provide the necessary power to accelerate or climb hills, but for the plain roads sections the engine size could be decreased, to provide better fuel economy. Auxiliaries considered with long-haul trucks can include for example refrigeration unit connected with the E-axle electrical system. This has actually already been demonstrated by SAF-Holland for example. (E-Mobility Engineering 2023) Another thing to consider related to all of these vehicle types is to see what the benefit could be for vehicles moving almost non-stop, so that the vehicle is only stopped for a moment during change of driver and refueling, hence all charging of the E-axle must happen during driving.

1.1.1 Downsizing And Fuel Efficiency

One of the interests is the downsizing of the engine while having additional power from the E-axle. Downsizing of an engine and thus lowering the overall performance of it, can allow it to shift operating point from higher specific consumption area to lower one. At the same time the overall performance of the vehicle is fairly unaffected because of the added power from the E-axle. In addition to downgrading, there might be possibility for further down speeding as well for some vehicle configurations, in which higher gear ratio transmission can be used since the electric machine assists the movement of the fully loaded vehicle and lower revving engine will naturally consume less fuel when optimized properly. (Huber 2018, p.822) The level of downsizing naturally depends on the size of the electric motor, so that its power must increase in proportion to the smaller engine. Down speeding will not be studied in this thesis, but the simulated vehicle will be tested with downgraded engine.

The Finnish legislation of road traffic act appendix 6.6(8.5.2020/360) states that a vehicle combination of over 44 tons must have at least 5 kW of power per each ton, so this has usually meant that certain engine sizes are necessary for 76-ton combinations. However, it also states that Traficom will give instructions of alternative means to show that the vehicle has adequate power. The same appendix also states that combination which uses alternative means of propulsion may have higher mass (over 76-tons) if the additional mass is due to alternative propulsion method. The maximum addition is 1000 kg and Traficom will give more detailed instructions of technical implementations that can be considered alternative propulsion method. From the legislative point of view the E-axle system seems feasible.

Another interesting aspect relating to downsizing is that E-axle could potentially provide additional traction force for gas operated timber truck for example, since gas engines typically have lower maximum engine powers compared to conventional diesel engines. Currently the maximum capacity of the first gas operated timber truck in Finland is 69t due to the limited engine power. (Niemi 2022)

1.1.2 Traction Improvement

Taction force improvement of the E-axle is based on the idea that it will provide additional torque and power which adds one additional driven axle to the combination. In order the get the vehicle moving on plain ground at least the force induced by rolling resistance must be overcome. (Birk et al. 2018, p.940–945) If every other aspect of the vehicle and road stays the same but one additional driven axle is added, it is clear that the overall ability of the vehicle to move over terrain will improve.

2 OVERVIEW OF HYBRIDS AND E-AXLES

According to EU directive 2007/46/EC, a hybrid vehicle is a vehicle which has two or more energy accumulators with their associated energy converters which drive the vehicle jointly or separately. Usually this means vehicle with internal combustion engine (ICE) paired with electric machine (EM). The way how these two are paired can vary a lot and the variations can generally be put into three categories: parallel hybrid, series hybrid and power-split hybrid drive. Hybrid vehicles can also be categorized based on proportion of electric power. The only interesting hybrid drivetrain type in this study is parallel hybrid, since as mentioned before, the E-axle trailer system is effectively parallel hybrid drivetrain when combined with a truck. If the trailer has ability to move on its own, then it will practically be a battery electric vehicle.

2.1 Parallel Hybrid and E-axle

In parallel hybrid drive both the ICE and the EM influence the movement of the vehicle simultaneously (parallel), but their functions are not directly related to each other, unlike for example in the case of a rigid axle between two different machine parts. Instead, both systems can operate individually of each other, such as when hybrid vehicle is able to drive solely on electric power, while the ICE is switched off. There are different ways to implement the EM in the parallel hybrid powertrain, and in passenger cars these different positions are typically named from P0 to P4, in which the number means position (from the front of the vehicle to the back) and P stands for parallel. This naming was originally developed by Daimler AG and has since been widely accepted nomenclature. The great advantage of parallel hybrid system is that it can be implemented to existing powertrain without major modifications or new transmission required. (Wafzig 2018, p.815) One good example is P4 parallel hybrid, also known as axle hybrid, in which EM is added to one of the vehicle non-driven axles, while ICE keeps directly powering the other axle(s) as usual.

The E-axle system considered in this thesis is effectively a P4 axle-hybrid, since all the functionalities of truck itself remain relatively unchanged, while the E-axle provides additional means of propulsion. Similarly, its position can vary on the different axles of

the trailer, but in practice its location must be chosen with driving stability and traction benefit in mind, but also axle masses need to be considered. The E-axle components need to be chosen and placed wisely in order to satisfy the requirements for axle masses but to also make sure the components are located in practical places on the trailer. Protection of the battery needs extra care in timber and tipper truck operations where there may be debris on the road. In fact, there are standards and regulations such as ISO 26262 for functional safety, which applies to electrical and electronic systems consisting of hardware and software (TÜV SÜD 2023). Another important regulation is ECE R100 which impose number of tests for testing battery systems found in electric powertrains (TÜV SÜD 2023). In overall, many regulations apply for development of E-axle, and even if that is not the scope of this study, it is good to keep in mind the need for complying many regulations.

2.1.1 Functionalities of the E-axle hybrid system

If it needs to be, all the typical hybrid system functionalities can be expected from the trailer-based E-axle system, which are (Huber 2018, p.822):

- Start/stop system to allow automatic starting and stopping of the ICE when the vehicle is driven solely on electric power such as in zero-emission zone in certain city areas.
- Recuperation to allow utilization of the regenerative braking, in which the EM converts kinetic energy to electrical energy, and thus saving energy otherwise lost in deceleration.
- Hybrid driving, in which the ICE and EM jointly drive the vehicle to allow best possible climbing or acceleration of the vehicle, or to assist movement in difficult terrain conditions. This mentioned capability is called boosting, but also generator mode should be realized, in which the EM is generating electricity by drag torque and thus the engine must use higher power to overcome the generator torque.
- External charging, so that the traction battery is not only charged by EM of the E-axle but can also be charged from mains electricity.

In practice, however, Start/stop system is not particularly feasible with trailer-based E-axle. The overall achievable efficiency and usability of the E-axle system is highly

depended on the E-axle control system, which takes care of managing the battery, driving and regeneration (and thus braking of the whole combination as well) of the EM. (Xue et al. 2020, p.1; Huber 2018, p.829) For example, the operation strategy of the E-axle must be able to consider the different ambient conditions. Too much regenerative braking on the E-axle might cause unexpected behavior on the trailer during winter when there is less grip compared to summertime, when the trailer is loaded differently or when the vehicle combination is in tight turn. The workings of the Anti-locking brake system together with the E-axle is also very important safety aspect. Depending on which axle on the trailer the EM is installed, it could push the combination in different ways if too much boosting from E-axle is provided. When discussing with drivers, a common wish was that E-axle should have manual mode so that the driver can have high control over the workings of the E-axle and thus the E-axle could be completely turned off at times if required.

2.2 Previous Studies on E-axle in HDV

Most of the studies related to E-axle in HDV application seem to circulate around the implementation in the vehicle and not so much about the system level use cases on different drive cycles and vehicles (Kieninger et al. 2019; Carnota 2020; EU Long Run 2020). In Carnota's master thesis for example, the E-axle is investigated from the perspective of vehicle manufacturer and pros and cons on how the E-axle could be implemented in the vehicle body is discussed. EU project Long Run and study by Kiesinger et al. (2021), were more focused on the design of the E-axle itself. The most closely related study to this was "*Investigation of Electrified Trailer Axles by Use of a Functional Model"* by Ritters et al., where simple measurement data from prototype E-axle semi-trailer was compared with simulations.

In this study the interest is in the overall possible potential what the E-axle could provide for different truck types operating on different drive cycles. The E-axle is considered on system level and design of individual components are of no interest. Electric machine on the E-axle for example will be modeled as a torque delivering component with tabulated values for performance and efficiency.

3 ELECTRIC DRIVE

The great advantage of EM over ICE is that it is simpler in design and can produce maximum torque from standstill, whereas ICE needs certain amount of engine speed to produce maximum torque. In this sense, the EM ideally supplements the ICE in vehicle propulsion and both combined can provide high dynamic response for every driving situation, not to mention EM is bidirectional, meaning that it can rotate in either direction. However, not all electric machines are same, just like not all internal combustion engines are same. Selection of suitable EM is selection between the best compromise just like with any machine. Typically, electric drive motors for vehicles are 3-phase AC (alternating current) motors and electric drivetrain fundamentally consists of battery, inverter, and the electric machine, which all must fit together as a one well-functioning group. (Alexander et al. 2018, p. 844; Huber 2018, p. 822–823; Kim 2017 p. 35; Nieminen 2020) Typically AC motors are reliable and have high torque density but require more complex control system than DC motors (Kim 2017, p.35). DC motors are typically not a choice of consideration due to their lower efficiency and higher maintenance needs, to name a few. The main objective in electric powertrain design is efficiency since better efficiency will allow use of smaller battery packs and simpler thermal management since less energy is wasted as heat. Next, let us investigate different properties of electric motors (AC) and how they affect the performance.

3.1 Electric Motor Properties

There are many important criteria for the selection of the electric motor such as size, cost, efficiency, overall reliability, and operating environment needs. In HDV use the motor must be as maintenance free as possible, since it will gain much higher mileage per time used than for example passenger vehicle and it will be used under heavy loads much more often as well. Ultimately simplified characteristic curve of an EM looks like Figure 1, in which area A is called base-speed area and area B is called field-weakening range. In the base-speed area the EM produces approximately constant torque and, in the field-weaking range approximately constant power is produced. This gives EM excellent acceleration from standstill. The operating points of the motor must always relay under this curve during use. The curve 1 in the Figure 1 is 60 s characteristics curve (overload curve) and

the curve 2 is continuous operation curve which the motor can achieve under certain determined conditions. If the motor was continuously operated at its limit such as the 60 s curve, at least one limit temperature of the system would be exceeded which would cause machine damage. (Alexander et al. 2018, p.844)

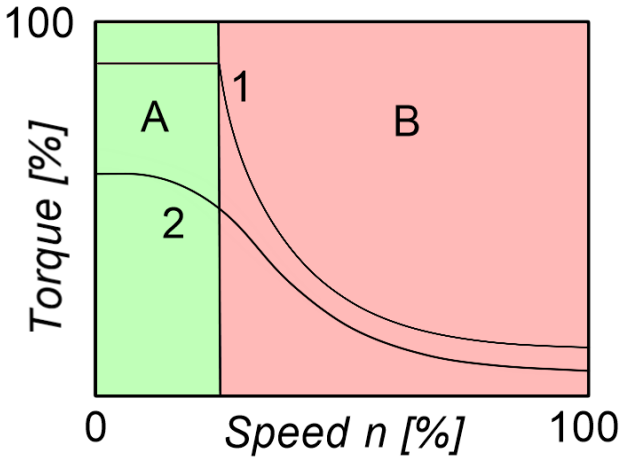

Figure 1. Characteristic curve of electric machines.

The maximum power and torque of the motor are independent of the thermal properties and are determined by the electromagnetic properties of the machine as well as supply current and voltage of the battery. The maximum limit characteristic curve of the motor would be above the 60 s curve. In order to achieve the best energy efficiency of the motor in the desired use case, the drivetrain should be designed in such way that the motor can operate in its most efficient area most of the time. Figure 2 shows example of EM efficiency map.

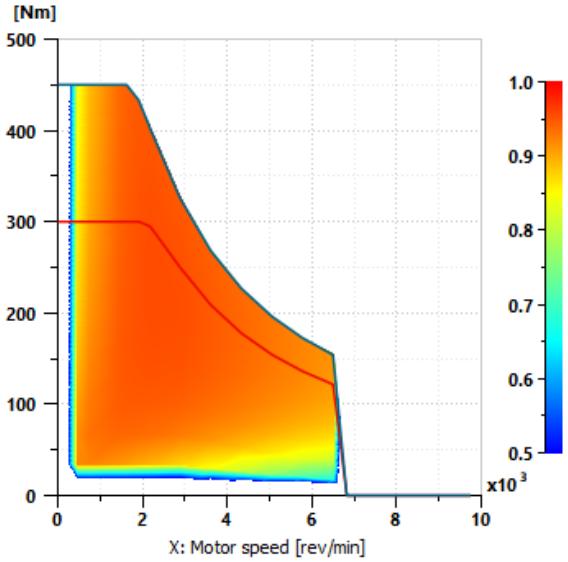

Figure 2. Example of EM efficiency map.

In this study, the interest of the EM lays on the overall performance side as a torque delivering device on a vehicle, so no deep investigation of EM calculation or simulation methods are considered. Efficiency for example can be calculated as a ratio between output and input power (Mäkelä et al. p. 92):

$$\eta = \frac{P_{out}}{P_{in}} \tag{1}$$

where P_{out} is the output power [W]
P_{in} is the input power [W] and
η is efficiency.

On fundamental level the mechanical power of EM can be calculated from torque and rotational speed as in any case, such that (Koch et al. p. 527):

$$P = 2\pi Mn \tag{2}$$

where P is engine power [W],
M is torque [Nm] and
n is rotational speed [r/s].

3.1.1 Operational Performance Influencing Factors

The maximum line-to-line voltage between EM and inverter increases the specific speed of the EM. Specific speed is the highest speed at the maximum torque, so in other words, higher voltage will shift the area A to the right (Figure 1). Voltage: however, has no effect on the maximum torque of the EM as that is determined by physical design of the machine parts. The maximum supply current of the EM influences the maximum achievable torque from it. In other words, higher current makes the curve go higher or lower in the speed-torque graph (Figure 1). With higher supply current the losses will also increase, which reduces the permissible overload time. The desired properties for the electric machine can be achieved by varying the dimensions, design, and material choices of the electric machine. (Alexander et al. 2018, p.849–855)

3.1.2 Losses

In electric machine, losses can be divided into ohmic losses, iron losses, eddy-current losses, and friction losses. In AC motor, friction losses appear only in the bearings and in the air gap between rotor and stator, as the air gets pushed around. In brushed DC motor friction losses would also appear from the contact of the brushes. Ohmic losses or copper losses are due to resistance in the wires. Iron losses occur due to rapidly changing magnetic field and eddy-current losses can occur in the magnet blocks of permanent magnet machines and in structural parts due to magnetic alternating field generated by the machine. Especially the eddy-current losses in the magnets are of particular importance, since the magnets are for the most part poorly connected to the cooling system and during high load the heat can lead to irreversible demagnetization. (Alexander et al. 2018, p.854–855; Oswos.com 2022)

3.2 Traction Battery

Battery is one of the most fundamental and important components of electric powertrain because it is the most limiting one for achievable performance and also expensive. The purpose of the battery is to store the required energy to operate the EM or other electrical components and to be able to provide high power for periods of time for example during acceleration. There are plenty of different battery technologies available these days, but

only a few of those are suitable or currently in use for electric powertrain, and the main reason for that are energy density and weight. Currently one of the most advanced battery technologies in use are Lithium-ion (Li-ion) batteries which are widely used in many applications ranging from mobile phones to electric vehicles. Also, as mentioned in section two of this thesis, many standards and regulations define how battery system should be made in automotive use to ensure safety. However, since deeper understanding of battery technology is outside the scope of this study, let us briefly discuss the overall characteristics of batteries from the perspective of Li-ion battery to have a little bit better understanding of them.

3.2.1 Overall Structure and Characteristics

Batteries are made of multiple cells connected in parallel and series to create a battery with desired values. In fact, multiple cells are packed together into a single unit called a battery module and modules are packed together to form a battery pack. Cells can be of different shapes and sizes, such as pouches, or cylindrical cases, which will affect the total size and shape of the battery. The voltage of battery pack is determined by the number of cells arranged in series with each other and thus depending on the cell properties, the total battery size increases with increased voltage level. The voltage level of the battery determines its power capability so that (Mäkelä et al. p. 120):

$$P = U * I \tag{3}$$

where, P is power [W],
U is voltage [V] and
I is current [A].

Greater current requires cables with larger diameter and generates more heat, hence the battery voltage should be raised higher and try to keep current levels low. Maximum current of the battery is determined by parallel connections between the cells. Estimated battery size can be calculated if dimensions of cells, battery voltage and estimated energy consumption are known. However, in reality, wiring, electronic circuits, cooling system casing etc. needs to be considered which will affect the final battery shape and size. (X-

engineering 2023; Benz et al. 2018, p.1324) In every battery, fade occurs over time, meaning that the overall performance of the battery decreases, such that for example, it will hold less charge or provide less power when used. (Han et al. 2019)

In overall Li-ion battery has a good energy density, long battery life, high lifetime cycle rate, high efficiency and it has no memory effect. Disadvantages are higher cost compared to other battery technologies, poor high temperature performance, and the need for protective circuits to keep the battery in operational area, when compared to other battery technologies. (Šimić et al. 2021, p.56; Benz et al. 2018, p.1324–1328) Currently typical energy densities for Li-ion batteries are around 50-270 Wh/kg which depends on the type of Li-ion battery (OSM Energy 2020; University of Washington 2023). Different types of Li-ion batteries are for example LFP (Lithium Iron Phosphate) or NMC (Nickel Manganese cobalt) which both have a little bit different characteristics and cost. In general, LFP has lower energy density but good safety properties and high lifetime while NMC offers better energy density but lacks in lifetime and safety. Also, LFP is cheaper than NMC, but still NMC has become increasingly popular due to its high energy density. In heavy duty vehicles LFP is still very much used due to its good life cycle properties. (IEA 2022, p. 138; Persun 2023)

3.2.2 Thermal Management

Thermal management of a battery is very important, since battery must operate in a certain temperature window, and the allowable thermal limits depend on type of battery technology. The lifetime of the battery reduces in increased temperature as many aging processes are temperature dependent. Also, if battery specific limits are exceeded exothermic thermal runaway is possible, which may be nearly impossible to stop once it has started. In cold temperatures the performance of the battery decreases and may completely fail to work. Two major types of cooling systems are typically used to cool batteries, liquid cooling, and air cooling. Liquid cooling is the most powerful cooling method, while air cooling needs 2 to 3 times more energy to achieve the same cooling result. Also, fin cooling system adds about 40 % extra weight. Liquid cooling system can also be built very compactly compared to air cooling system. (ACS 2022; Dragonfly

Energy 2022; Benz et al. 2018, p.1329) Battery management system monitors the temperature, voltage and current, both in cell level and overall level and carries out balancing to keep cells' state of charge in check. Information from the battery management system is sent to vehicle control units responsible for the control of the power electronics to configure operations (Benz et al. 2018, p.1327).

3.2.3 Modeling a Battery

Developing a realistic battery model is a complex task due to complex behavior and numerous interactions that take place in it, thus there are many different approaches how to model batteries, such as electrochemical, electrical equivalent circuit model and experimental model. Equivalent circuit model consists of basic electrical components such as resistors and capacitors and aims to simulate the electrical behavior of the battery and give good balance between accuracy, complexity, and calculation time. Electrochemical model simulates chemical effects in the battery and thus is not of interest on this level of investigation. (Tremblay, Dessaint, Dekkiche 2007, p.1; Hedon 2018, p.20–21)

Since the interest of this thesis is not about what is exactly happening inside the battery, a generic battery model is to be used. In Simulink Simscape Electrical library there is a system level battery model which represents generic self-discharging battery, and which according to MathWorks is sufficient for modeling in medium-level fidelity for drive cycle analysis. (MathWorks 2023a)

3.3 Inverter Unit

In its simplest, inverter takes in the DC power from the battery and converts it to AC to drive EM or in the case of braking recuperation, converts AC from EM to DC into battery. Thus, inverter is key component for efficiency and performance of electric powertrain. Strictly speaking, inverter is a device that provides AC from DC source, but inverter is also common term for EV component which does that and more. (EatonVideos 2020; Omron 2023) Inverter changes the speed of the EM by varying the AC frequency and increases or decreases the torque/power by adjusting the voltage. However, changing between AC and DC causes losses which creates heat, so inverters require cooling system

and thermal management to avoid damages. It does not matter what the performance specifications are for battery and motor if inverter unit is not also capable of delivering desired levels of performance. Typically, EMs have greater thermal mass than inverters, so inverters are typically the limiting factor when it comes to heat problems. (Boyd 2022; E-mobility Engineering 2023)

Besides of battery, electric machine and inverter, there are other components in the electric powertrain as well, but since in this thesis the interest is on system level E-axle, there is no need to go into details of the powertrain components. However, these three components are key components of electric powertrain which allow energy flow between energy source (battery) and drive unit (electric machine). (E-vehicle Info 2021; Power Electronics News 2023)

4 VEHICLE DYNAMICS

Simulations of a vehicle is based on vehicle motion equations. Handling of a vehicle consists of dynamics of longitudinal (in direction of X-axis), transverse (in direction of Y-axis), and vertical motion (in direction of Z-axis). Transverse motion deals with the steering of the vehicle, while longitudinal motion deals with acceleration or braking behaviour, and vertical motion deals with excitations caused by road irregularities. The motion of the vehicle body can generally be considered rigid body, since deviation from the rigid body motion only occur above frequency range of 10 to 15 Hz. (Dragon 2018, p.930) The vehicle coordinate system used in this study is the ISO 8855 coordinate system as shown in Figure 3.

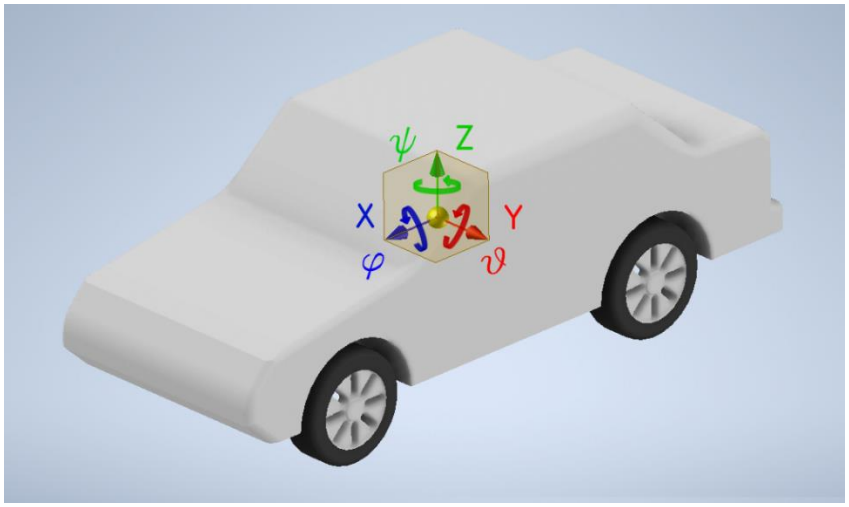

Figure 3. ISO 8855 based coordinate system.

4.1 Dynamics of linear motion

In vehicle simulations when the interest is for example in energy expenditure, power, acting forces for drive operations, or developing control logic, a longitudinal model (linear motion) of the vehicle is enough. Longitudinal simulation is comparable to dyno measurement and thus has its limitations on accuracy, but on the other hand, it is accurate enough when the steering dynamics of the vehicle is of no interest and the road surface is smooth enough, so that bouncing movements of the vehicle body can be disregarded. One example of such dyno run is WLTP (Worldwide Harmonised Light Duty Vehicle Test

Procedure) testing used for passenger vehicles to determine their consumption and pollution levels and the same run can be simulated if the necessary vehicle parameters are known. Simplified longitudinal vehicle model is shown in Figure 4, where the resisting the forces are show.

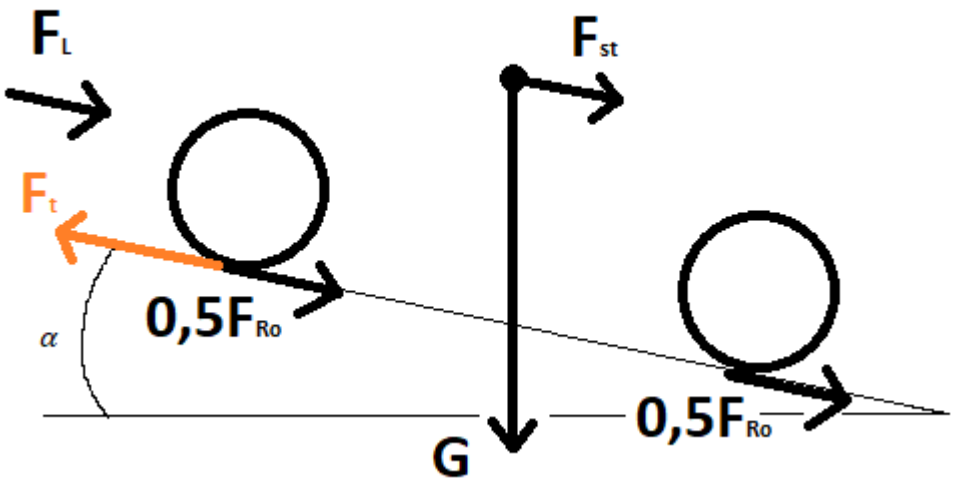

Figure 4. Resisting forces on a longitudinal vehicle body.

The vehicle combination in this study is represented by lumped mass model *m*, in which trailer mass is included to the vehicle model and centre of gravity in X-direction is summed. When the trailer and vehicle are simulated and treated as one single unit, it does not matter whether the E-axle is in the trailer or in the vehicle in the real application since they both affect to the movement of the same body. Obviously, in real life there is always some amount of relative movement between the truck and the trailer since real machines will always have clearances. The powertrain supplies tractive force F_t on the driven wheels, and driving resistances resist the movement of the vehicle. Driving resistances or total running resistance F_w consists of aerodynamic drag F_L, climbing resistance F_{St}, and rolling resistance F_{Ro}. This can be denoted as (Birk et al. p. 941):

$$F_w = F_{Ro} + F_L + F_{St} \tag{4}$$

The required power at the driven wheels to overcome these resistances is (Birk et al p. 941):

$$P_w = F_w * v \tag{5}$$

, where P_w is total running resistance power [W] and
v is the vehicle speed [m/s].

The rolling resistance F_{Ro} is caused by the deformation processes which occur between the tire contact patch and the road surface. The rolling resistance coefficient can be empirically determined. The following applies to rolling resistance (Birk et al p. 942):

$$F_{Ro} = f_R * m * g * \cos\alpha \tag{6}$$

, where f_R is rolling resistance coefficient,
m is vehicle mass [kg],
g = 9,81 [m/s^2] and
α is gradient angle [deg].

According to Bosch automotive handbook 10th edition, the coefficient of rolling resistance is directly proportional to the level of deformation and inversely proportional to the radius of the tire. (Birk et al., p. 941) Thus the coefficient will increase in response to higher loads, higher speed, and lower tire pressure. Same is mentioned in Theory of Ground Vehicles 4th edition by Wong on page 8. Resistance due to circulating air on the surface of the tire is also mentioned, but its contribution to rolling resistance is said to be minimal.

The aerodynamic drag is calculated as shown below (Birk et al p. 942):

$$F_L = \frac{1}{2} * \rho * c_w * A(v + v_0)^2 \tag{7}$$

where ρ is air density [kg/m^3],
c_w is drag coefficient,
A is cross-sectional area of the vehicle [m^2],
v is speed [m/s] and
v_0 is headwind speed [m/s].

Aerodynamic drag power can be calculated similarly to equation (2). The climbing resistance is calculated as (Birk et al p. 943):

$$F_{St} = m * g * \sin\alpha \tag{8}$$

The tractive force available at driven wheels of a vehicle can be calculated as (Birk et al. p. 944):

$$F = \frac{M*i*\eta}{r} \tag{9}$$

where M is engine torque [Nm],
i is overall transmission ratio,
η is total drivetrain efficiency and
r is radius of driven tire [m].

Atmospheric conditions affect air density ρ, and therefore aerodynamic resistance. For example, warm is air is less dense than cold air or going high enough in the elevation will also cause drop in air density. (Wong 2008, pp. 223) The cross-sectional area of the vehicle is the area which goes along the direction of movement e.g., front of the vehicle. This area can be calculated for example by directly taking measurements, from good photograph or by other means such as 3D model. If the air drag coefficient isn't known, it can be determined either experimentally by coast down tests, or by wind tunnel testing if such is available. (Wong 2008, pp.224–225; Birk et al. 2018, pp. 941–943) It is also notable to mention that the aerodynamic coefficient c_w depends on the truck combination yaw angle as well. It is shown in Wong – *Theory of Ground Vehicles* -book 4th edition at page 236, that at least up to a yaw angle of 15°, the coefficient increases. This however is not considered in the creation of the vehicle model since the model is going to be longitudinal, but it is still good to understand the limitations of simulation model.

4.1.1 Load distribution and weight transfer

Load distribution of the vehicle along X-axis is simply a function of the vehicle geometry. If the front axle of the vehicle is considered origin, the total center of mass can be calculated from the axle masses as a function of distance as usual. The total center of mass then lies between the axle masses. The vehicle combination will be modeled as 2-

axle models, so that only the driven axles are modeled. The front axle of the vehicle model will be considered the truck's driven axle and the rear axle will considered as the trailer axle where the E-axle would be installed. Wheelbase will be determined for each vehicle from the center of the truck's rear bogie to center of the determined axle in the trailer. Basically, for each trailer type, the E-axle is considered to be installed in the front axle(s) based on the idea of better driving behavior. Since the simulations in this study will be done in ideal conditions so that slip won't occur, the effect of axle masses is not important here. Weight transfer caused by the center of gravity is not simulated and thus bounce and pitch motion of the vehicle are disregarded as well.

4.1.2 Fuel economy and losses

The fuel economy of a vehicle depends on many factors, such as engine fuel consumption characteristics, transmissions characteristics, vehicle weight, aerodynamic drag, rolling resistance, drive cycle and driver behavior. Effect of driver behavior is much smaller in simulated vehicle since it simply tries to follow reference speed profile and does it exactly the same way each time, if parameters have not changed. Vehicle weight is also not considerable factor when focus is on heavy duty vehicles since the point of such vehicles is in an essence to move detachable mass from one place to another, and thus higher the delivered mass, the better the overall performance. From the engine perspective, the fuel economy is always better with lower engine speeds and higher loads, compared to high engine speeds and low loads. In order to minimize fuel consumption, vehicles and especially HDV are configured so that the engine stays on the most efficient area as much as possible. (Wong 2008, p.281)

Another considerable factor affecting fuel economy of a vehicle are losses in the drivetrain. Most losses happen in the internal combustion engine since modern heavy duty compression ignition engines have maximum efficiencies up to around 50 % while overall drivetrain efficiencies can be estimated to be around 80–90 %. (Birk et al. 2018, p.944; Rahkola 2018, p.11; Scania 2021; Bosch 2020)

5 CREATING THE VEHICLE MODEL

The vehicle models were created with MATLAB version R2023a in Simulink, using both Simscape driveline and Simulink libraries to create them. Some simulations or related matters were also done in Siemens Amesim (version 2021.1) -simulation software. On the fundamental level the vehicle consists of two main blocks which are the driver and the vehicle block as shown in Figure 5. Auxiliary blocks were gearbox control logic (GCL) (down in the Figure 5) and in the E-axle model also the motor control logic (MCL) (in the upper part in Figure 5) which determines the usage of the E-axle.

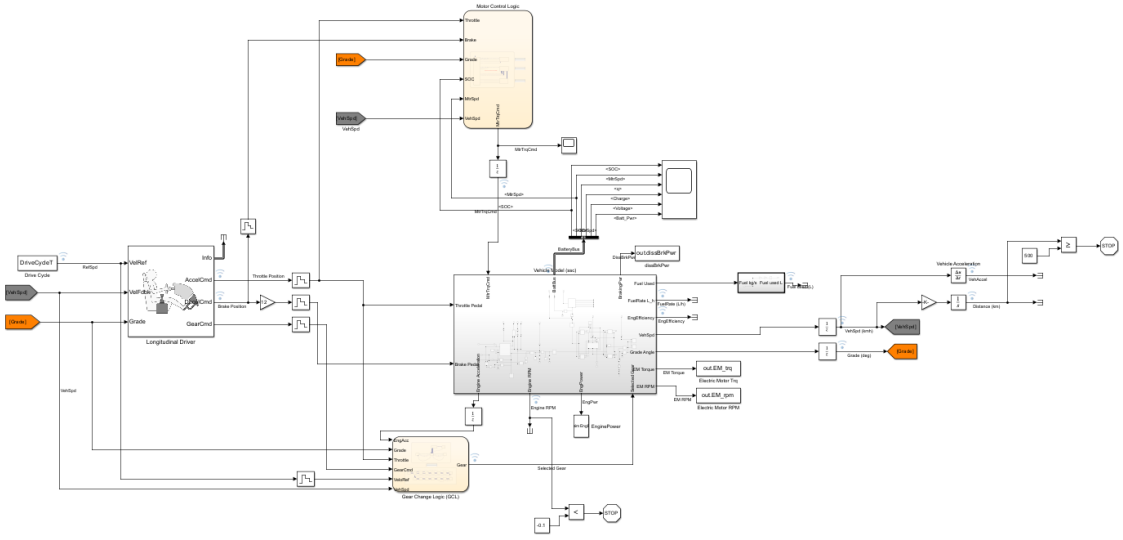

Figure 5. The overall look of the vehicle model with E-axle.

The model is forward-facing vehicle model which means that there is a driver model which controls the accelerator and brake pedals of the vehicle in order to try to follow desired drive cycle speed that is inputted to the model, and inevitably there is always a small margin of difference between the desired speed and achieved speed. The torque from the engine that the driver model controls, proceeds along the drivetrain with losses to the wheels and road profile where the resistance forces are calculated. This is similar to real world situation where vehicles are tested on dyno rolls and the driver tries to achieve the desired speed profile. This sort of model is well suited for hardware and control simulations because it simulates measurable quantities in the drivetrain (Wipke, Cuddy and Burch 1999, p.5).

This sort of model is dynamic and more realistic in a sense than backward facing vehicle model, in which speed is not dynamic variable but instead the vehicle is assumed to be able to achieve the desired speed and the performance of all components are calculated based on this speed through the drivetrain from wheels to engine. This sort of model calculates faster than forward facing model but is not well suited for dynamic simulation. (Wipke, Cuddy and Burch 1999, p.4–5)

5.1 Driver Model

The driver model used was "*longitudinal driver*" block from Simulink library and is parametric speed tracking controller for generating normalized throttle and brake signals, ranging from 0 to 1, based on reference and feedback velocities. The reference velocity comes from example logged vehicle data. The control type was PI with shift type of "Reverse, Neutral, Drive". This shift type would not have been necessary and didn't affect the workings of the model but was left-over in the model after some other early tests. Velocity feed-forward, grade angle feed-forward and anti-windup parameters were set to zero. (MathWorks 2023b)

5.2 Vehicle Model Components

The vehicle model was created using Simscape Driveline block set and consists of generic engine block along with disc friction clutch, generic transmission block and simple gear ratio to represent final drive, through which torque is provided to front axle of the longitudinal vehicle model block.

5.2.1 Engine Model

The engine block represents configurable internal combustion engine which is suitable for both diesel and gasoline engine applications (MathWorks 2023c). The engine is controlled by normalized throttle signal (between 0–1) and was parameterized with tabulated torque and speed data and fuel consumption was calculated from brake specific fuel consumption (BSFC) table which was generated in Siemens Amesim Engine Maps Generation tool. The efficiencies for the engines were set to around 46 % in the Engine Maps Generation tool. However, BSFC map is not perfect for fuel consumption

simulations since when the engine is dragging and not producing torque and thus not consuming fuel, the BSFC will approach infinity since it is calculated as (Koch et al. 2018, p.528):

$$b_e = \frac{B}{P_{eff}} \tag{10}$$

where b_e is BSFC [g/kWh],
B is fuel consumption [g/h] and
P_{eff} is engine power [kW].

The infinity problem can however be alleviated by setting limits to the table extrapolation values.

The vehicle specific values are shown under section “Vehicle specific information”. The torque curves for each engine were obtained from open-source information such as vehicle brochures provided by Scania. Inertia for the engine was set to 16,6 kgm^2 for the 16,4L V8 engine and 15,6 kgm^2 for the 12,7L I6 engine. Engine inertia was approximated by looking at the acceleration speeds of the simulated engine with gearbox on neutral from idle to full speed. Idle speed was set to 500 rpm and stall threshold to 200 rpm. The engine is modeled with starter, since it was found that the model was more stable if the engine was not running right from the start but is instead started in the beginning of the simulation. The starter consists ideal torque source with step function to give enough torque for period of time to start the engine.

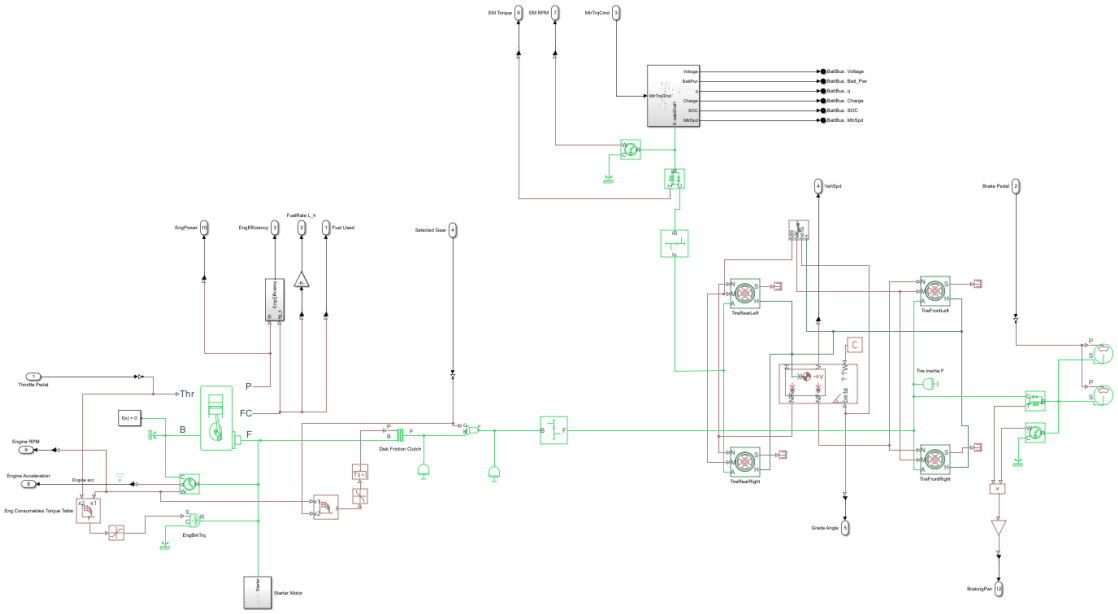

Figure 6. Layout of the ICE Simscape vehicle with E-axle.

In Figure 6 we can see the layout of the ICE vehicle model, consisting of engine on the left and vehicle body on the right. The green line from the engine is physical connection from engine crankshaft through transmission components to a driven axle and tires. In the ICE vehicle model the front axle is driven by engine and the rear axle is free axle, representing axle on the trailer. In the E-axle model the rear axle is connected with the electric machine and corresponding E-axle components.

Power taken by auxiliaries were modeled by a lookup table with torque values so that the power would stay constant throughout the engine speed range. Some engine brake torque was also added in the same table for times when throttle pedal, which is also directly engine load, was less than zero. The reason for this was that the behavior of the engine was simply not satisfactory without the brake torque, especially in very slow vehicle speeds or during higher decelerations.

Fuel consumption is automatically calculated by the generic engine block in units of kg/s so couple of calculation blocks were added to convert the consumption into units of l/h. Engine efficiency is calculated from engine power and fuel consumption according to equation (Koch et al. 2018, p.528):

$$\eta_e = \frac{P_{eff}}{BH_u} \tag{11}$$

where η_e is engine efficiency,
P_{eff} is engine power [W],
B is fuel consumption [g/s] and
H_u is fuel specific calorific value [MJ/kg].

Ideal rotational measurement block was also connected to the engine model in order to measure engine speed for monitoring and debugging purposes.

5.2.2 Clutch, Transmission and Final Drive

Clutch was modeled with Simscape "*disc friction clutch*" block which was controlled by lookup table consisting of clutch pressure as a function of engine speed. No losses were modeled in the clutch. Friction model for the clutch was "*fixed kinetic friction coefficient*".

After the disc friction clutch block is Simscape "*transmission*" block which takes in the gear ratio as a Simscape physical signal input. Gear ratio of the vehicle transmission are parameterized in MATLAB script from which the transmission block reads the set gear ratio array values automatically from 1 to n starting from the first value in the array. 0 value represents neutral position and -1 represents reverse. Gear shift type was set to instantaneous since it was thought that for concept level and system level study the small time needed for gear shift did not have any meaningful effect for the representation of whole model. Also, this way there was no need to model throttle blip during gear shift. Even though transmission block also models a clutch, it was not used for the purpose of the vehicle's actual clutch, since it only worked with on/off principle and made moving from standstill difficult.

After transmission block is "*simple gear*" block, which represents final drive of the vehicle. Basically, since friction levels for both tires are exactly the same and only longitudinal motion of the vehicle is simulated, the need for separate block for final drive was not necessary. However, adding a separate block makes the model visually more

comprehensible. The final drive ratio was determined in the vehicle script which had all the values for the simulated vehicle. The overall efficiency of the drivetrain was set to 0,9. Without measured data or other accurate information, this was thought to be in somewhat reasonable range, but most likely a bit optimistic for a truck with double-drive bogie. In this way the transmission also had only one constant for the efficiency, instead of separate efficiencies for each gear.

Some inertias were also added to the drivetrain in order to account for rotating masses. Between clutch and transmission is inertia of 0,81 kgm^2 and between final drive and transmission is inertia of 2.44 kgm^2. values were obtained from Petter Lundberg's Master's Thesis "*Investigation of the transient nature of rolling resistance on an operating Heavy Duty Vehicle*" from page 53 and the vehicle used in that study was similar to the vehicles used in this E-axle study.

5.2.3 Vehicle body, Tires, Brakes and Road profile

Vehicle body was modeled with Simscape "*vehicle body*" block. Block represents a two-axle vehicle body in longitudinal motion. The block accounts for vehicle mass, air drag, road grade and weight distribution between the axles. Pitch and bounce dynamics of the vehicle body were not modeled, and the vehicle does not move vertically relative to the ground, but always follows the ground profile perfectly. Gravitational acceleration was typical value of 9,81 m/s^2. Frontal area, drag coefficient and air density were defined in MATLAB script of the considered vehicle. The aerodynamic drag of the vehicle is modeled through the vehicle center of gravity, but when pitch motion is not accounted for, the aerodynamic drag force does not cause moment to the vehicle body. The vehicle body block is assumed to be in pitch and normal equilibrium and assumes that wheels never lose contact to the ground which may cause negative normal forces. (Mathworks 2023d)

Tires were modeled with Simscape "*tire*" blocks and were friction parameterized in terms of static and kinetic friction. Static friction determines the applied torque at which the tire loses grip and kinetic friction coefficient determines the amount of torque that the tire transmits after it begins to slip. Slip output type was relative, roll radius and rolling resistance were defined in vehicle script file and inertia was only modeled for front axle

which was the truck driven axle. Inertia and rolling radius for one tire of size 315/70R22.5 were 14,9 kgm^2 and 0,492m respectively. (Lundberg 2014, p.53, MathWorks 2023e)

Brakes were modeled with Simscape "*disc brake*" blocks. Even though in simulation model one brake block would have been enough, two brakes were used on the vehicle driven axle for the sake of visual comprehension. Only the front axle of the vehicle body was modeled with brakes. The rear axle, which was considered trailer axle, had no brakes but was only braked by the EM of the E-axle system when E-axle was simulated. Brake was controlled by Simscape pressure physical signal, which was routed from the driver model's normalized brake signal which was multiplied in order to provide adequate pressure.

Simscape road profile block was used to input elevation profile for the simulated drive cycle. Different friction conditions along the driven route of the simulated vehicle were also possible to input from the road profile block but was not used.

5.3 Gear Change Logic (GCL)

The logic to control gear change in the simulated vehicle is automated and is based on lookup table consisting of vehicle speed as a function throttle position and gear number. There were two separate tables, one for down shifting and the other for up shifting. The gear change logic (GCL) was created in MATLAB Stateflow and is shown in Figure 7. The basic working of the GCL is quite simple, so that gear is changed when threshold speed has been passed for a period of time. Some multipliers were added, and their values altered for different vehicle combinations in order to allow different gear change behavior in up hills. This due to not realizing well enough in the beginning when model building was started, that how great effect the GCL has for the movement ability of the loaded truck combination. However, there was no time to build better control logic, and this logic proved to work reasonably well after all.

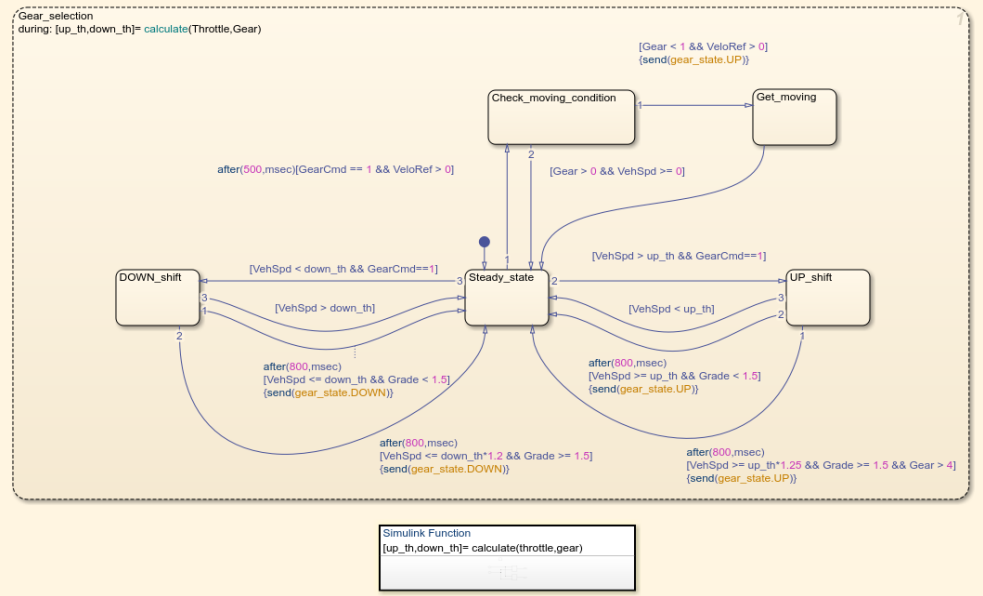

Figure 7. Gearbox Control Logic.

In Figure 8 are shown the gears that the gear change logic can change to. Every vehicle in this study happened to have 14 speed transmissions so the same base model could be used for each vehicle. In the logic are also transitions which allow jumping over some gears. The simulated vehicle will always initially start with 1st gear, but when certain conditions are met it will jump directly to 3rd gear which is basically the 1st gear of high range in the real gearbox. During normal drive cycle simulation, low gears are only used during start of the movement from standstill and majority of the time gear number is higher than 4. The use of gear command to switch from neutral to first was not necessary for this model but was left there from early model which had a little bit different control logic. It did not affect the overall workings of the model.

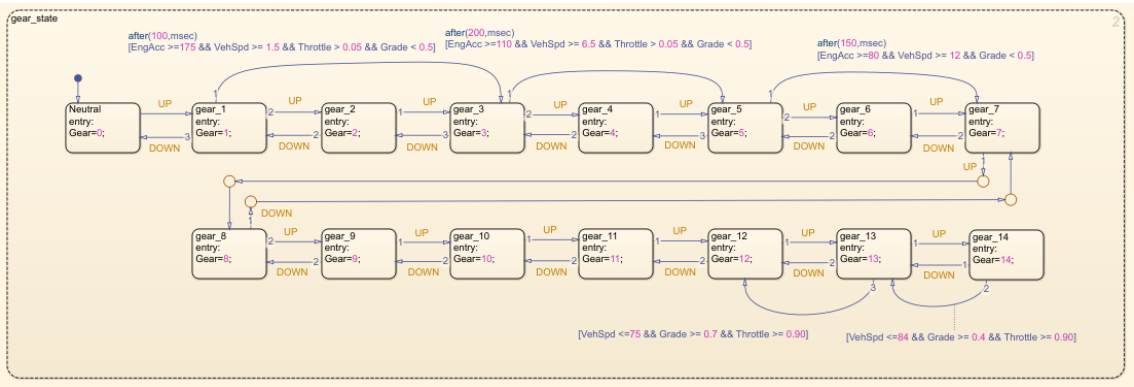

Figure 8. The gears in the Gear Change Logic.

5.4 Motor Control Logic (MCL)

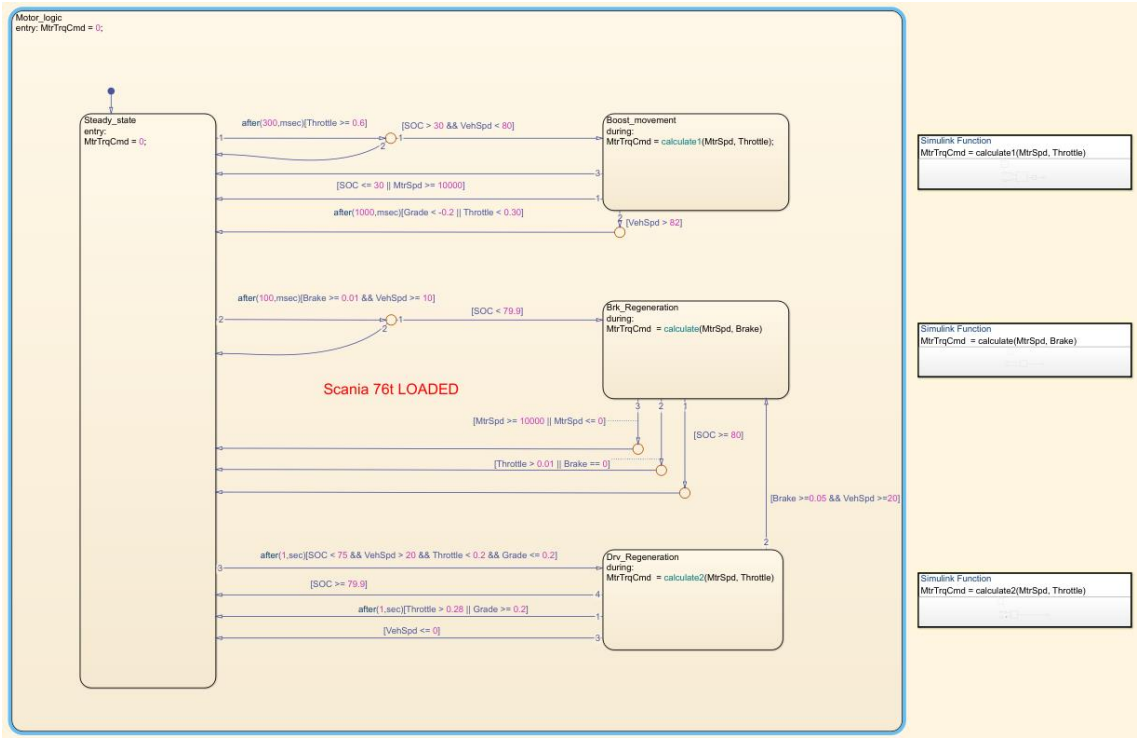

Figure 9. Motor Control Logic.

The control of the electric motor on the E-axle was created on MATLAB Stateflow similarly to GCL. The motor control logic (MCL) is entirely reactive and is based on pedal positions, battery state of charge (SOC), vehicle speed, road grade and electric motor rotational speed. By altering the parameters of the transitions seen in Figure 9 it was possible to get different results with the E-axle in terms of battery usage, regeneration and boosting and fuel used during simulated drive cycle. The control strategies for the boosting, brake regeneration and drag regeneration were lookup tables consisting of EM torque as a function of EM rotational speed and pedal position. For the sake of better comparability and to keep the number of variables in reasonable levels, the MCL settings were kept the same for each vehicle, after satisfactory settings were found in tests. This of course affects the achievable performance from E-axle.

5.5 E-axle components

The overall layout of the E-axle is shown in Figure 10, consisting of Simscape "*battery*" block, "*DC-DC converter*" block and "*motor & drive (system level)*" block. On the right of the model are measurements related to battery, such as SOC, battery power and voltage level.

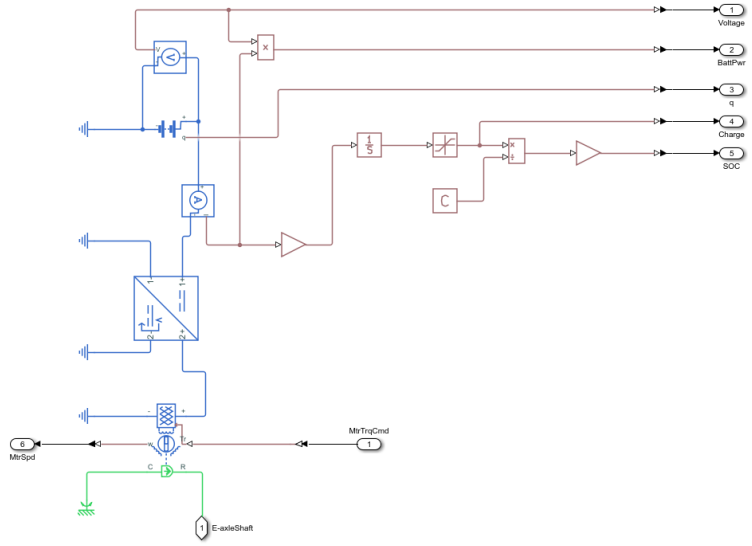

Figure 10. Layout of the E-axle components.

5.5.1 Electric Machine for the E-axle

As mentioned, the motor was modelled with Simscape "*motor & drive (system level)*" block, which represents generic motor and drive operating it torque-mode and is suitable for system level traction motor simulations (MathWorks 2023f). The motor torque range is defined by tabulated torque envelope with speed with allowed intermittent over-torque. Allowed over-torque limit was 30 s with 60 s cooldown. Torque control time constant (Tc) was kept in Simulink default value of 0,02 s, which is the reaction time of the motor output torque in respect to demanded reference torque. Rotor inertia was set to 0,05 kgm^2 and the motor model works with DC current.

In the selection of EM for the E-axle, size and torque were two main criteria for the choice, because too big EM cannot be fitted into the body of a trailer. Specifications for the EM were based on BorgWarner liquid cooled Permanent Magnet Synchronous motor

platform 240 with 500 Nm continuous torque (BorgWarner 2023). It was chosen as it seemed to have the highest torque in compact size, compared to other manufacturers. The motor attributes were created in Simcenter Amesim since Amesim's Electric Motor Tables Creator -tool could predict the overall characteristics of electric motor reasonably well, when continuous base power, maximum continuous torque, maximum speed, ratio between continuous and peak torque, motor type and cooling are inputted. From Amesim the motor specs were brought to MATLAB. The motor torque curve is shown in Figure 11 and the colour gradient presents losses in kW. The motor was simulated without losses when it was free coasting, but when it was either regenerating or boosting, the losses followed values shown in Figure 11. In other words, the EM losses were tabulated values consisting of losses in kilowatts as a function of rotational speed and torque. The motor was operated at 700 V and had gear ratio of 12:1 with efficiency of 0,97. With the gear ratio of 12:1, the EM would operate approximately at highest of 5500 rpm, so as can be seen in Figure 11, the usable range consists mostly of the area of the best efficiency and torque.

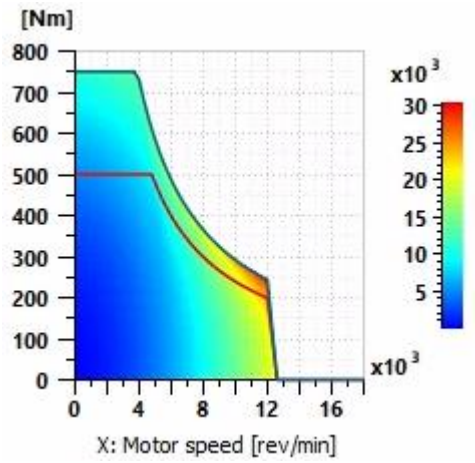

Figure 11. Torque curve and losses for the used electric machine.

5.5.2 Battery model

The traction battery for the E-axle system was modeled with Simscape "battery" block, without self-discharge, charge dynamics, fade, aging, or thermal properties. Internal resistance for the battery was constant 0,11 Ω, nominal voltage 840 V and tested nominal capacities were 20 kWh, 35 kWh and 50 kWh. The battery size was a choice of balance

between being small enough not to be too expensive or bulky and having enough energy to make some sense in use. Thus, three different battery sizes were chosen with 15 kWh step size, which was thought to give an idea about the potential of the chosen battery size. The battery's no-load voltage versus SOC is shown in Figure 12. According to the battery model's documentation page, this sort of battery model provides medium level fidelity for hybrid and electric drivetrain drive cycle analysis (MathWorks 2023a). Battery usable SOC was determined to be between 80–30 % which is approximately typical range for batteries rated for longevity (Mahajan 2020; Battery University 2019), while many sources state that typical usable SOC for traction batteries is around 90–20 % or similar, depending on the battery system (Faßnacht 2018, p.1309; Geotab 2022). The range of SOC is, however, not crucial from the perspective of the final results in this study, since the used range is known and stays the same for each and every simulated run while the nominal battery capacity varies between 20–50 kWh.

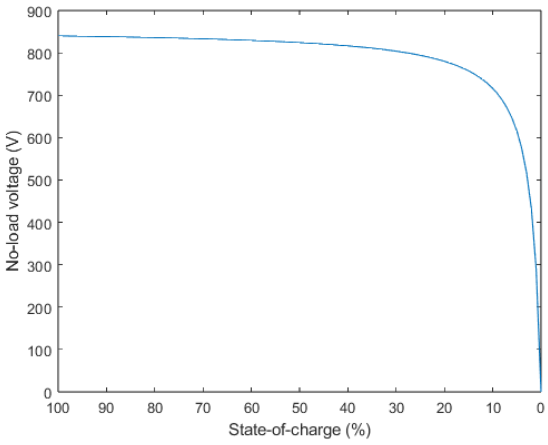

Figure 12. Battery model no-load voltage vs SOC.

5.5.3 Inverter model

Inverter for the E-axle system was modelled with Simscape "*DC-DC Converter*" block with extremely low converter losses at zero output power and with efficiency of 0,98 at the rated output power. Rated output power was set to 350 kW and reference voltage demand to 700 V which is the voltage level for the EM to use. No dynamics or thermal effects were modeled for the inverter. The block regulates voltage on the load side and draws required amount of power from the input side to balance input and output power

and losses. The block is modeled bidirectional, so that it can support regenerative power from the load site to supply side, such as in the case of regenerative braking operation. (MathWorks 2023g)

6 DATA COLLECTION AND VEHICLE INFORMATION

In order to get specific information about the vehicles and especially their drive cycles, the vehicles were logged with universal CAN loggers with GPS. With timber truck the GPS data was also combined with inertial data, which provided excellent accuracy of the road profile. Loggings took from weeks up to a month, depending on how there was time and possibility to keep the loggers in the measured vehicles. Logging frequency was generally 10Hz and the logged data was exported to MATLAB's MAT-file format in order to be used in Simulink. In general, every channel possible was logged, in order to get enough information, and later only the channels necessary for the simulations were chosen and exported to MATLAB.

All of the three vehicle types used in this study happened to be Scania. The long-haul truck was Scania R540 6x4, the timber truck was Scania R660 8x4*4 and tipper truck was Scania R730 10x4*6. The transmission on timber and long-haul trucks were the same G33 transmission while tipper truck had GRSO925. This information is based on the gear ratios which was logged from the vehicle CAN bus. The gear ratios for G33 are shown in Figure 13 and the gear ratios for GRSO925 are shown in Figure 14. Figures 15, 16 and 17 show the engine torque curves and figures 18 and 19 show used BSFC maps for the simulated engines. Engine torque curves were created with MATLAB, based on freely available information from Scania. The BSFC maps, as mentioned before, were created in Siemens Amesim, since no real data was available. Areas which are not possible to reach in the BSFC map, have constant value from the last possible reachable value. Also, in the low engine speed range, the values are not meaningful, since the engine rarely operates in that area but instead mainly operates above engine speed over 800 rpm. Basis for the vehicle resistance parameters were found from study "*Raskaan kaluston VECTO-simulointi Suomessa"* by Pekka Rahkola. All other information about the vehicles were found from various online sources and freely available information provided by Scania.

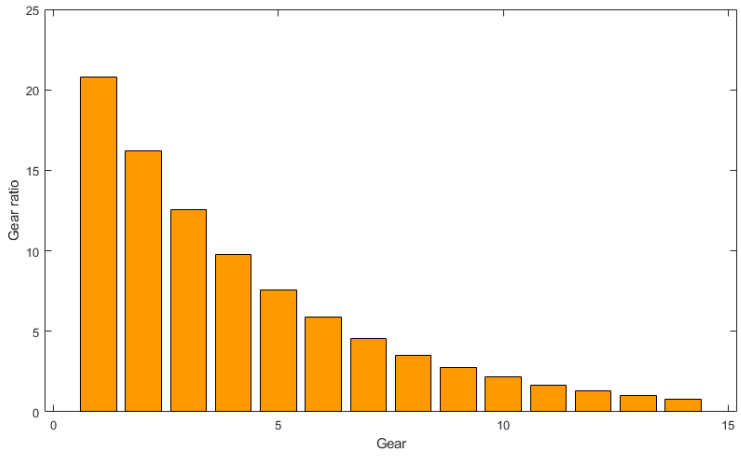

Figure 13. Gear ratios of G33 transmission.

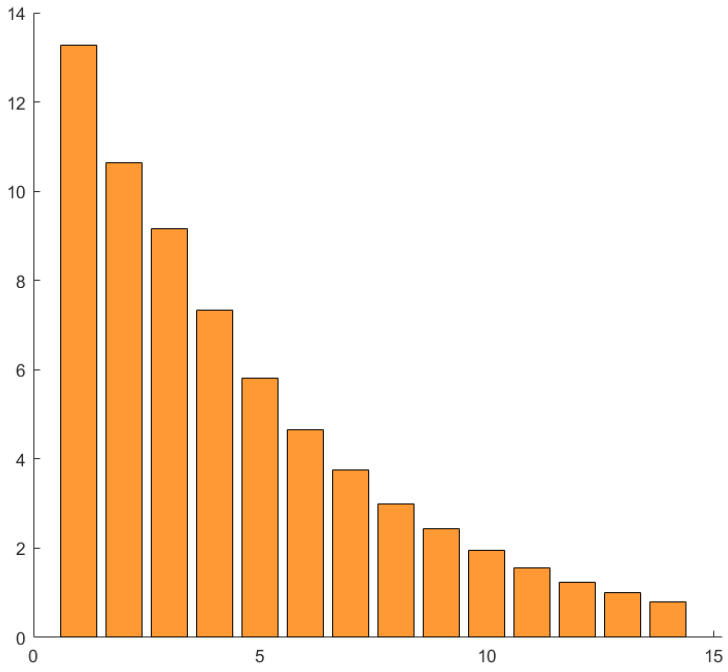

Figure 14. Gear ratios of Scania GRSO925 transmission.

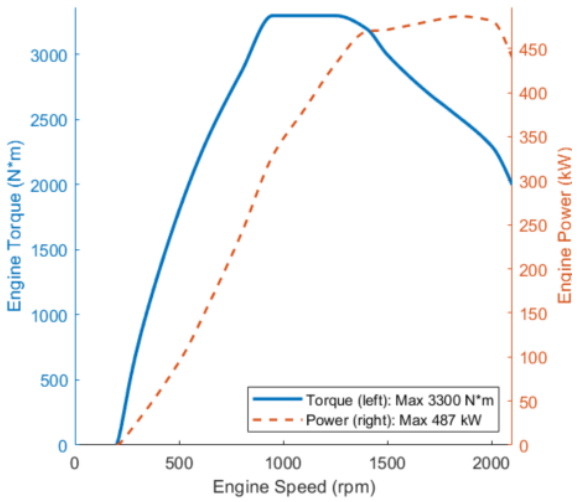

Figure 15. Power and torque curve of the Scania R660 16,4L V8 engine.

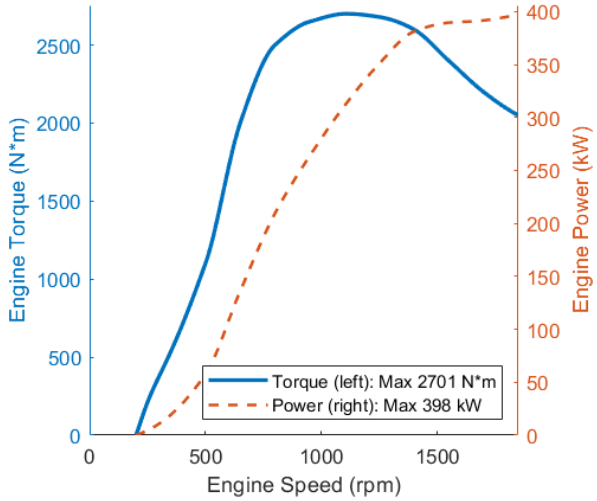

Figure 16. Power and torque curve of the Scania R540 12,7L I6 engine.

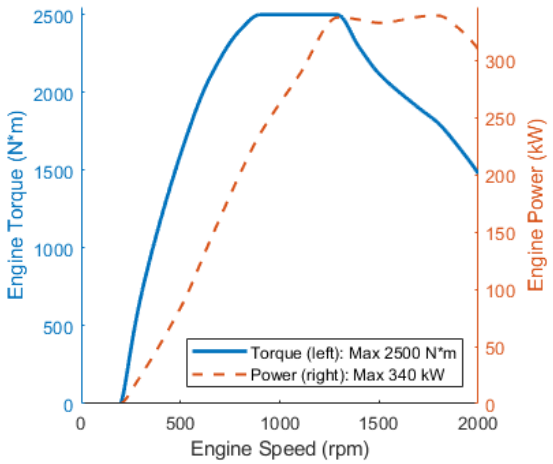

Figure 17. Power and torque curve of the Scania R460 12,7L I6 engine.

Torque_FC

Eng_speed

		1	2	3	4	5	6	7	8	9	10
		65	**480**	**977**	**1309**	**1641**	**1973**	**2304**	**2719**	**3051**	**3300**
1	**200**	473.80	480.40	450.30	420.30	330.30	320.30	318.30	316.30	312.5	300.5
2	**500**	473.80	222	201.40	196.30	193.20	193.20	193.20	193.20	193.20	193.20
3	**650**	542.20	232.5	204.30	200.10	195.60	193.80	192	192	192	192
4	**800**	616.5	240.20	210.90	203.90	198	194.40	191.70	189.40	189.10	189.10
5	**950**	687.80	250.60	215.60	207	200.80	196.60	193.70	191.10	189.60	185.5
6	**1100**	759.10	260.30	220.40	210.60	203.5	198.90	195.60	192.80	190.10	189.5
7	**1250**	806.70	266.80	223.5	212.80	205.30	200.40	196.90	193.90	192.10	191
8	**1400**	901.80	282.40	229	217.10	208.90	203.20	199.30	196.10	194.10	193.30
9	**1500**	949.40	288.10	232.10	219.80	211.10	204.80	201.5	197.20	195.70	195.70
10	**1700**	1044.5	301.40	239	223.80	215	208.30	203.30	199.20	199.20	199.20
11	**1800**	1092.10	308.20	242.40	226	217.10	209.20	204.80	201.90	201.90	201.90
12	**2000**	1113.90	314.40	247.20	230.5	221.40	213.40	208.90	205.90	205.90	205.90
13	**2100**	1169.60	330.10	259.60	242	232.5	224.10	219.30	216.20	216.20	216.20

Figure 18. Simulated BSFC map for the R660.

Torque_FC

Eng_speed

		1	2	3	4	5	6	7	8	9	10
		50	**729**	**1001**	**1205**	**1408**	**1613**	**1749**	**2089**	**2428**	**2700**
1	**200**	480	480.40	450.30	420.30	330.30	320.30	318.30	316.30	312.5	300.5
2	**500**	513.5	205	198	194.90	192.40	190.20	189.10	189.10	189.10	189.10
3	**650**	550	210.10	202.30	200.20	195.60	194.30	194.5	190	190	189
4	**800**	680.10	215.60	206.20	202	197.80	195	194	191.10	189.30	188.40
5	**950**	791.10	224	212.5	206.30	201.90	198.70	196.90	193.70	191.40	186.10
6	**1100**	846.60	227.80	215.30	208.60	203.80	200.40	198.5	195	192.5	185.10
7	**1250**	957.60	235.5	220.70	213.10	207.70	203.70	201.60	197.60	194.80	186.10
8	**1400**	1013.20	240.60	222.90	215.10	208.90	206.20	202	197.60	196	195.10
9	**1550**	1124.20	245.90	227.30	219.90	214.40	208.90	206	201.80	199.30	199.30
10	**1700**	1179.70	250.70	229.30	222	216.5	210.90	207.70	202.80	202.80	202.80
11	**1850**	1235.20	254.10	234.30	224.10	217	212	209.60	204.60	204.60	204.60
12	**2000**	1272.30	261.70	241.30	230.80	223.5	218.40	215.90	210.70	210.70	210.70

Figure 19. Simulated BSFC map for the R540 and R460.

6.1 Timber Truck

Timber truck was tested with the actual 660 hp 16,4l V8 engine but also with 12,7l I6 540 hp and 460 hp engines of which the 460 hp engine represents gas powered engine in terms of engine performance. In the case of 660 and 540 versions, only the engine parameters were changed. With 460 hp, also final drive ratio was altered, but the same fuel map was used as for 540 hp engine. With 460 hp engine the main interest was about the movement ability of the vehicle and less about the fuel consumption. Timber truck was tested both empty (26t) and loaded (76t). In the loaded simulation, the E-axle had full battery and in the case of empty vehicle, the battery was at minimum level. The purpose of this was to see if it is possible to charge the battery from empty to full by driving, since timber trucks are often operated around the clock and in such areas, that there is no real possibility to charge the battery from mains electricity. The torque curves for 660, 540 and 460 engines were as shown in Figure 15, Figure 16 and Figure 17 respectively.

Vehicle parameters for timber truck:

- Rolling coefficient: 0,0062 (for empty and loaded)
- Drag coefficient: 1,536 (empty) 1,426 (loaded)
- Air surface area: 9,96 m^2
- Mass: 76 000kg (loaded) 26 180kg (unloaded)
- Air density: 1,341 kg/m^3
- Rolling radius: 0,492 m
- Final drive ratio: 2,71:1 (3,08 for 460 hp engine)

Air density depends on the temperature of the logged day, but only one value is shown here.

6.2 Long-haul Truck

Long-haul truck was simulated with its normal 540 engine as well as downgraded 460 engine. For 460 simulations, also the final drive ratio was changed in addition to engine parameters, otherwise everything else stayed the same. Similarly, to timber truck, the battery was full in the beginning of simulation for the fully loaded (76t) truck and empty in the beginning of the simulation for the unloaded (24t) truck.

Vehicle parameters for long-haul truck:

- Rolling coefficient: 0,014 (loaded) 0,006 (unloaded)
- Drag coefficient: 1,055
- Air surface area: 9,96 m^2
- Mass: 76 000kg (loaded) 24 000kg (unloaded)
- Air density: 1.292 kg/m^3
- Rolling radius: 0,492 m
- Final drive ratio: 2,85:1 (3,08 for 460 hp engine)

6.3 Tipper Truck Specifications

Tipper truck was simulated with its normal 730 engine as well as downgraded 540 engine. For the sake of simplicity, only the engine was changed, all other parameters of the vehicle stayed the same. Similarly to timber truck and long-haul truck, the battery was empty in unloaded drive cycles and full in the loaded drive cycles.

Vehicle parameters for tipper truck:

- Rolling coefficient: 0,0068 (loaded) (0,0072 unloaded)
- Drag coefficient: 1,212 (loaded) (1,352 unloaded)
- Air surface area: 8,50 m^2
- Mass: 76 000kg (loaded) 24 000kg (unloaded)
- Air density: 1.268 kg/m^3
- Rolling radius: 0,507 m
- Final drive ratio: 3,8:1

7 CONDUCTED SIMULATIONS AND RESULTS

Simulations consisted of validations runs and the actual E-axle test runs. In validation runs the logged data was compared with simulated vehicle without E-axle in order to make sure that the simulated vehicle represents the actual vehicle well enough, and the in comparison runs the E-axle was added and assisting in the movement of the vehicle. In E-axle assisted simulations, the battery was full at the beginning of the fully loaded vehicle simulation and empty at beginning of the unloaded vehicle simulations. Empty battery at the start of unloaded vehicle simulation was used, to see if it is possible to get battery full by driving when stopping for charging isn't an option. Suitable drive cycles were chosen from the logged data and then used for the analysis of the vehicle specific simulations. Generally speaking, timber and tipper truck drive cycles were shorter in distance and consisted of more fluctuation in the vehicle speed than long-haul truck, which drive cycle consisted mostly of constant speed driving with much lower frequency of decelerations and accelerations. The one-way distances for tipper truck were from couple of kilometers up to about 100 km, and for timber truck the distances were around 100 km and for the long-haul truck the distances were about 340 km. The long-haul truck was operating on the same route all the time.

In additions to simulations based on logged data, much more simple performance test simulations were also done, where the comparison of E-axle vs ICE only is much clearer. Acceleration tests were carried out on plain ground profile by setting reference speed to 82 km/h so that the vehicle would immediately try to reach that speed, and once 82 km/h was reached, the simulation would stop. Acceleration time could then be examined. Another test consisted of 25,5 km test route with elevation profile as shown in Figure 20. Reference speed was once again set to 82 km/h, with optimal friction level so that no slip would occur, and vehicle would try to keep that speed level throughout the test. Fuel consumption, time, used pure energy/work in engine and lost energy in brakes were then examined. Hill climbing ability of ICE vs E-axle was also tested with reference speed of 75 km/h, to see how hill affects vehicle speed.

7.1 Results from Performance Tests

As mentioned, the performance of the E-axle vs ICE only was tested with drive cycle consisting of constant 82 km/h reference speed for 25,5 km with road profile as shown in Figure 20 and friction levels with no slipping occurring.

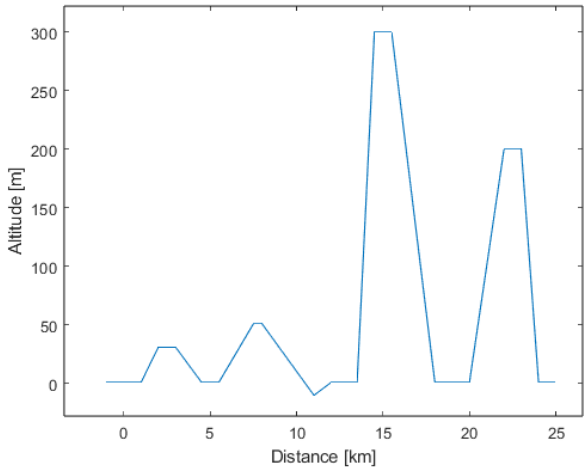

Figure 20. Road profile for performance tests

Lost energy due to braking was examined via Simscape “disc brake” block, to see how much less braking energy was used when E-axle was in use. The control parameters for the MCL were same throughout different tests. Certainly, if MCL parameters were changed, or if the whole control logic was different, different results would be seen. Also, more accurate electrical model would also likely affect the results shown here. However, results shown here give a good idea of the potential of the E-axle versus ICE in ideal conditions.

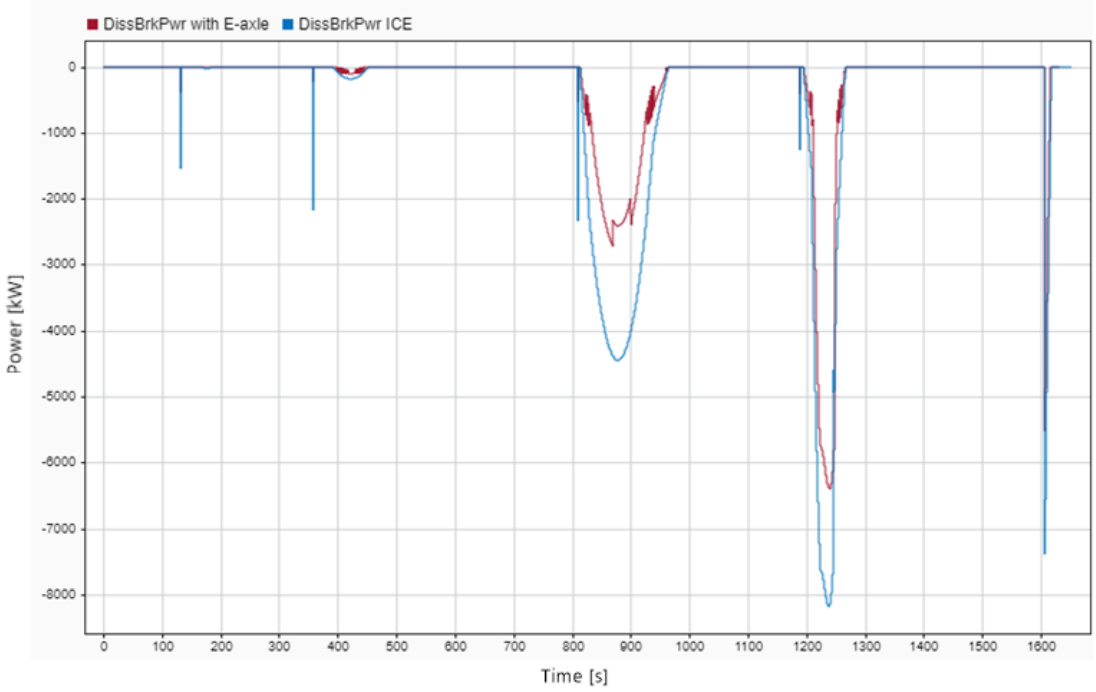

Figure 21. Curve shows braking power in kilowatts with ICE only and with E-axle.

Figure 21 shows the difference in braking power in kilowatts between vehicle with E-axle and vehicle without E-axle. From the power, energy can be calculated so that, with ICE only, the vehicle used 2,14 kWh in the brakes and with E-axle 1,28 kWh was used. This gives approximately 40 % reduction in energy lost in braking. Similar results were observed in the logged drive cycle-based simulations, with results varying approximately between 20–60 %. The drive cycle profile of course has an effect on the braking power, because depending on the drive cycle, the use of brakes may be higher or lower.

In Figure 22 are shown R660 timber truck results with E-axle vs ICE in the road profile presented in Figure 20. Fuel used with ICE only was 29,6 *l* and with E-axle fuel used was 24,2 *l*, thus decrease in consumption was 18,2 %. Time used to reach 25,5 km for the ICE only was 1569 s and with E-axle it was 1505 s, thus E-axle assisted vehicle was 64 s (4,1 %) quicker. Pure energy consumption (not fuel energy) or work done in engine was 126,9 kWh with ICE only, and 101,1 kWh (-20,3 %) with E-axle. For the electric motor boosting the energy was 28,4 kWh, which corresponds to decrease in engine energy when losses are considered. Battery capacity was not limiting factor in this test, as the interest was to see what the pure difference between E-axle and ICE is when electrical energy is not limiting performance. When battery had finite charge and set to 20 kWh (Figure 23),

consumption was 26,2 *l* (-11,5 %), engine work 109,4 kWh (-13,8 %) and time used 1558 s (11 s quicker). The results with 20kWh battery are shown in Figure 23.

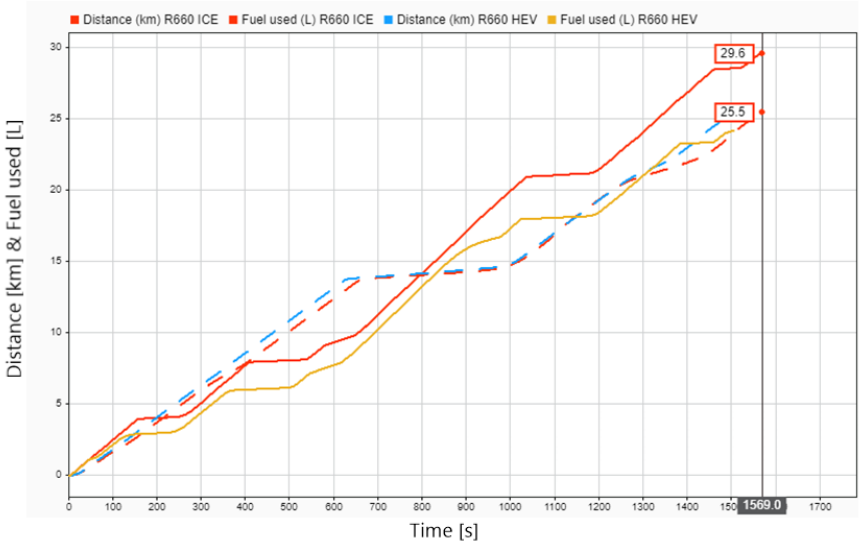

Figure 22. Performance test for R660 ICE vs E-axle. Battery not limiting. Dashed line is for distance in kilometers.

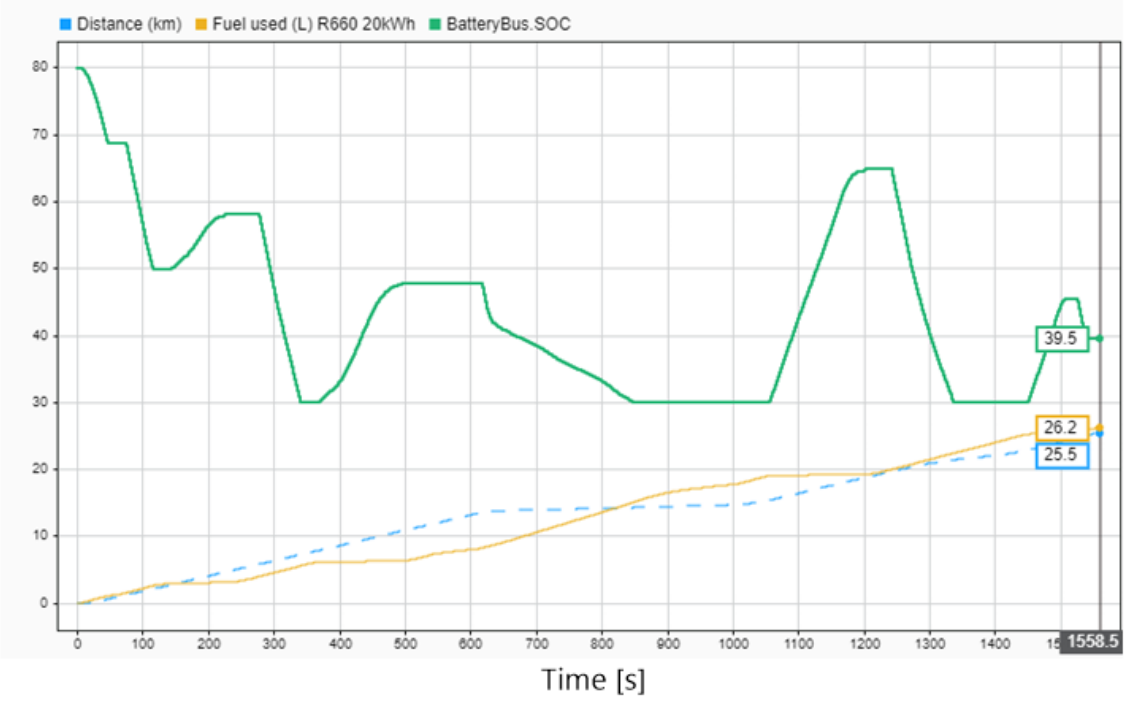

Figure 23. Results with R660 E-axle with 20 kWh battery.

Same test was also carried out for the R540 long-haul truck and results between ICE and E-axle are shown in Figure 24. Similarly, to R660, battery was not limiting factor in the test. Results with R540 ICE only were: fuel consumption 30,3 *l*, time used 1714 s, work done 128,8 kWh. With E-axle the fuel consumption was 24,1 *l* (-20,5 %), time used 1667 s (-47 s or 2,7 %) and energy used 98,8 kWh (-23,3 %) Results show similar gains with the E-axle which is expected since the E-axle configuration and control logic are exactly the same and only vehicle specific parameters differ. Different vehicle parameters cause a little bit more usage of the EM in boosting. In Figure 25 the map of torque points for EM is shown for R540 long-haul during these tests. Map for R660 is not shown, since both vehicles have E-axle configuration with same control logic, so the maps are very much identical.

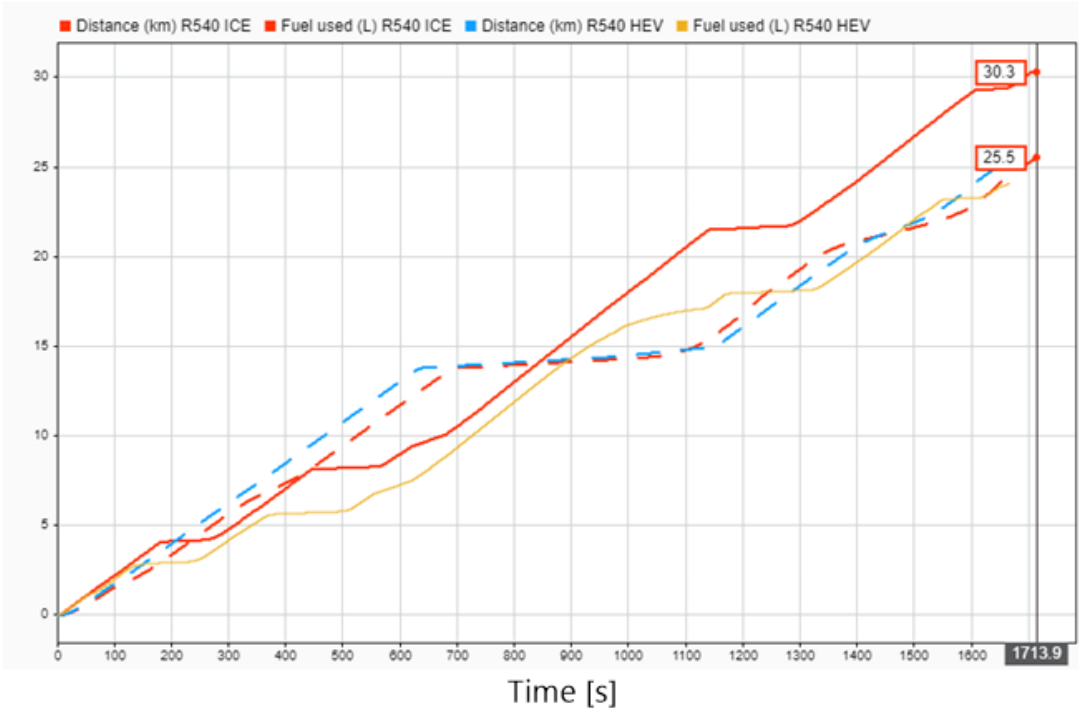

Figure 24. Performance test results for R540 long-haul with E-axle. Dashed line is for distance in kilometers.

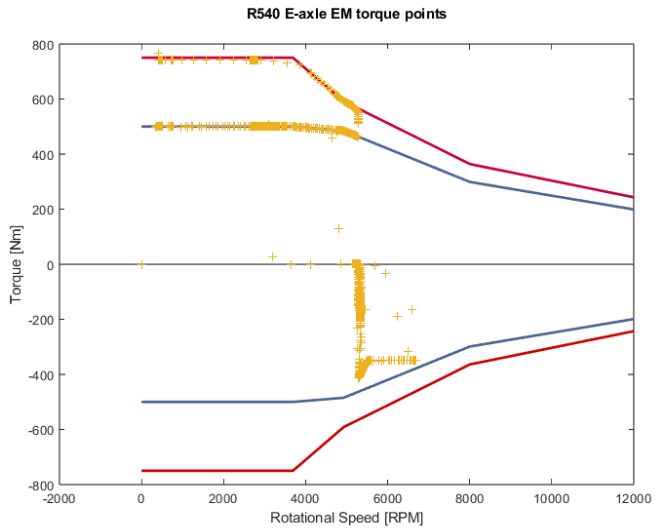

Figure 25. EM torque points with R540 long-haul.

For R660 the torque map looks exactly the same in shape, but it has a little bit fewer points of usage due to higher engine power and the same control logic used.

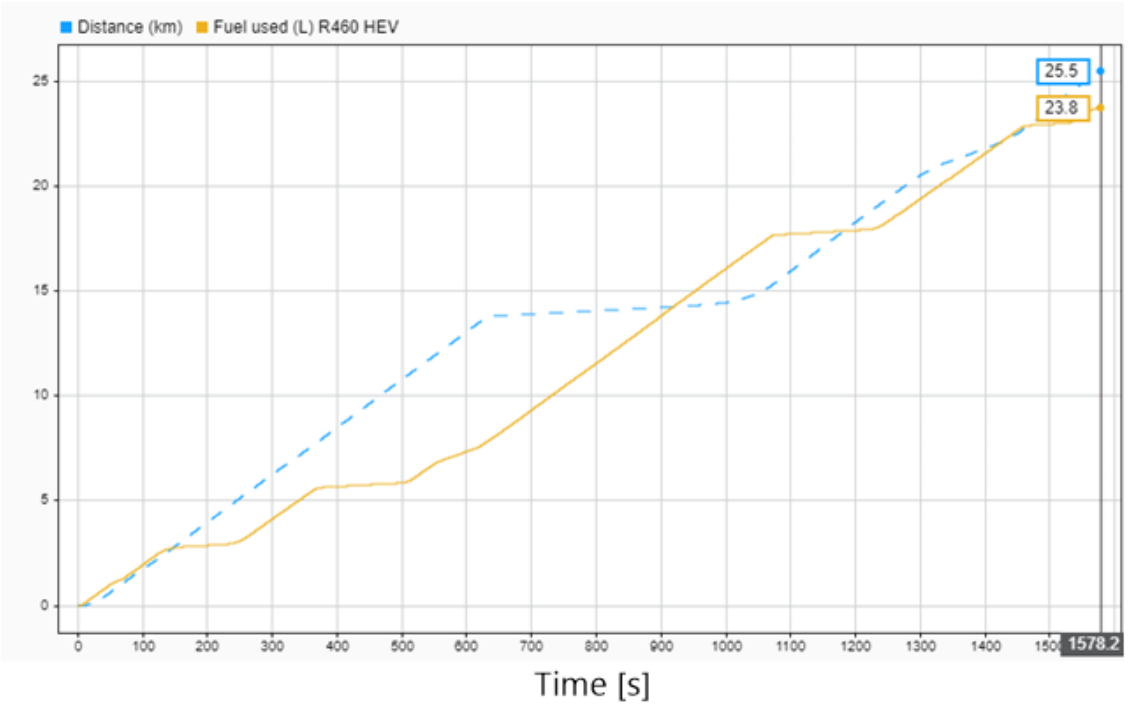

Figure 26. Performance test result for R460 with E-axle.

For R460 with E-axle the results are shown in Figure 26. The R460 was not tested without E-axle because 460 hp engine is not of real interest for 76t combination since the engine is underpowered by the law. Fuel consumption was 23,8 *l* (- 19,6 %), work done 96,1 kWh (24,3 %) and time used 1578 s (9 s slower). Results show similar performance with R660 with ICE only, which gives a good idea of the potential of E-axle with downgraded engine. Changes in brackets are comparison to R660 ICE.

7.1.1 Hill Climbing Ability and Acceleration

For hill climbing ability estimation, the traction force of each vehicle was calculated. Calculations were done at 75 km/h for easier comparison, since at this speed engine of each vehicle is still in the highest torque range and the E-axle is also producing the continuous 500Nm torque. Traction forces for different vehicle configurations are shown in Figure 27, from which it can be observed that the E-axle roughly doubles the traction force at 75 km/h. In the figure, T stands for timber, L stands for long-haul and G stands for tipper or gravel truck.

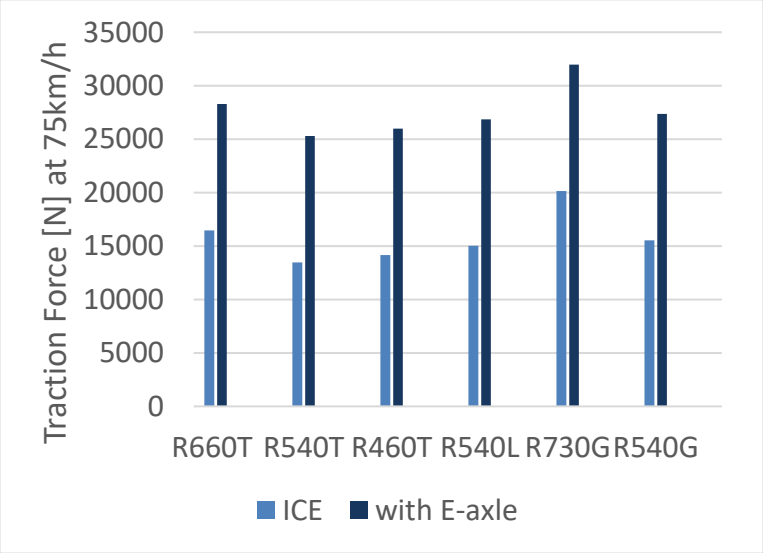

Figure 27. Traction force differences.

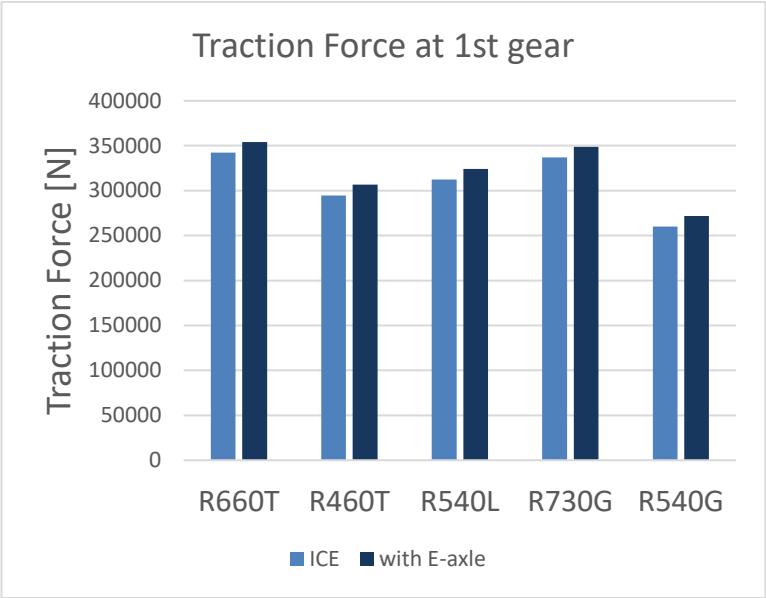

Figure 28. Traction force at 1st gear.

In Figure 28 is comparison of traction force in 1st gear, where it can be seen that the effect of the EM is much smaller than in road speed (gain is less than 5 %), which is mostly because the EM has constant gear ratio. If it had for example 2-speed gearbox, there could be low- and high-speed ranges for road speed and crawling speed.

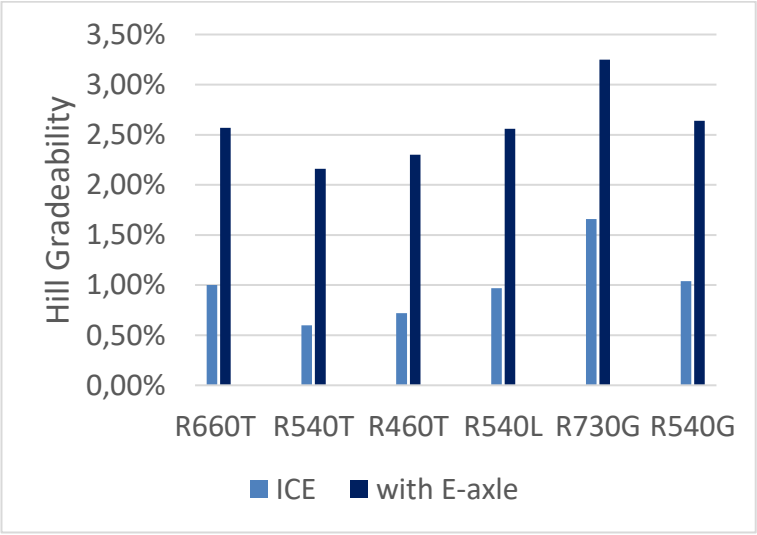

Figure 29. Hill gradeability for different configurations.

When traction force is compared with overall climbing resistance, it can be seen (Figure 29) that also the hill gradeability is roughly doubled at 75 km/h. It can also be seen that with E-axle, if battery energy is not considered, the overall performance of the vehicle with downgraded engine at road speed in hills, greatly exceeds that of regular vehicle with ICE only. All the vehicles in Figure 27, Figure 28 and Figure 29 were calculated with same parameters, so that only engine parameters changed, except for R460. Also, only R460 timber specifications are shown in the figure because the specifications for R460 long-haul would be almost exactly the same, since they both have same transmission and final drive ratio, and only vehicle resisting forces would differ.

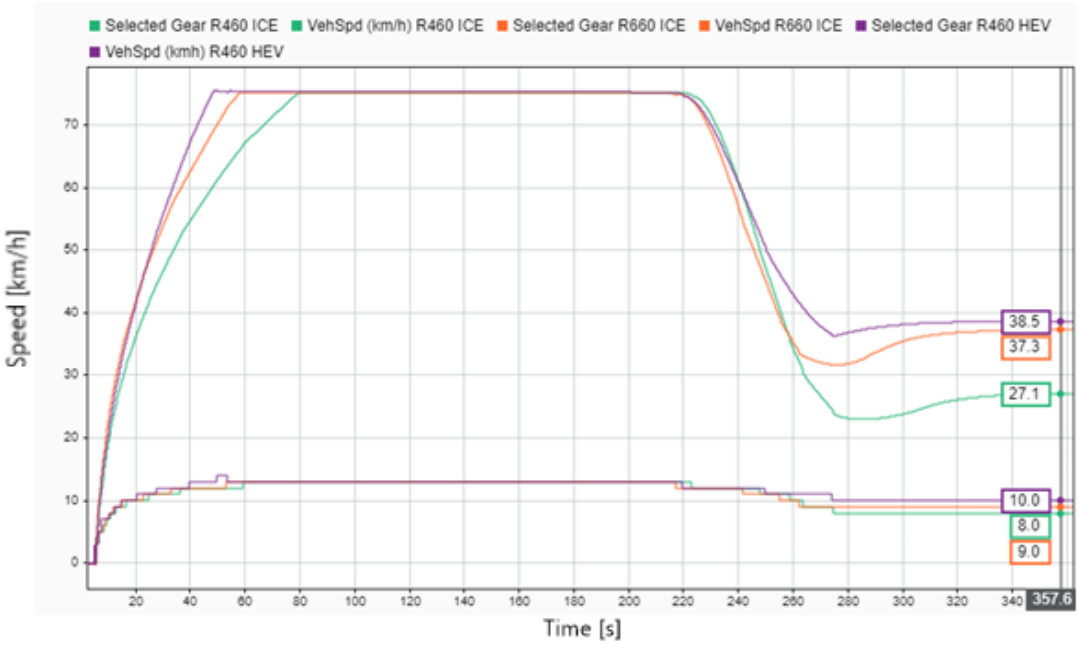

Figure 30. R660 ICE vs R460 E-axle vs R460 ICE in 5 % hill.

In Figure 30 is shown difference in speed in 5 % hill between R660 ICE, R460 ICE and R460 with E-axle. 5% hill is over the limits for each vehicle at 75 km/h and 13th gear, but it can be seen that with E-axle, the R460 quite closely matches that of R660 with ICE only, whereas R460 ICE is clearly underpowered. Each was simulated with 76t weight in order to show better comparison even though 76t is over the mass limit for regular 460 hp truck combination. R460 with E-axle continues in the hill with 10th gear whereas R660 ICE uses 9th gear and R460 ICE uses 8th gear, clearly showing the increased traction force due to E-axle. The difference in speed in hill between E-axle and ICE only seen in Figure

30 applies to every combination, as shown in Figure 29 as well. Only with increased vehicle overall power, the base speed achieved in the hill differs, but the relative change between ICE only and E-axle will remain relatively same, according to Figure 29. The power requirement at constant 82 km/h on flat surface between R660 and R460 timber is shown in Figure 31. In the simulated vehicle the throttle position is directly proportional to engine load, thus engine load increases approximately 21,6 % on flat surface between R660 and R460 on the same gear, based on the values used in these simulations. Between R540 and R460 long-haul, the increase in engine load was 4,7 % for R460. The throttle position shown in Figure 31 is the normalized throttle position of the simulated engine, where value of 1.0 corresponds to 100% and 0 to 0%.

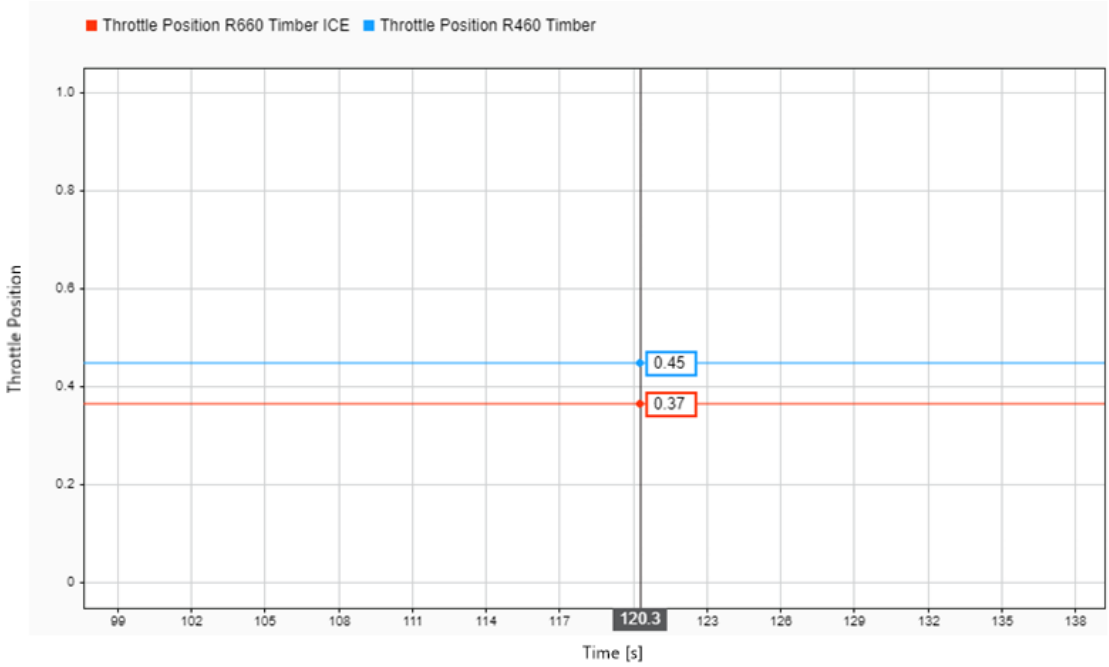

Figure 31. Engine load difference between R660 and R460.

Acceleration of each vehicle was simulated between 0–82 km/h with and without E-axle assistance. Results are shown in Table 1. With larger engine size and thus power, the difference between ICE only results and E-axle assisted results gets smaller, which is logical since the proportional share of the total power between EM and engine gets smaller as well.

Table 1. Acceleration test results.

	R460 Long-haul	R460 Timber	R540 Long-haul	R540 Timber	R540 Tipper	R660 Timber	R730 Tipper
ICE only (s)	93,0	90,6	82,4	74,7	78,4	67,2	54,8
with E-axle (s)	50,9	50,1	47,6	45,1	46,8	41,6	37,3
difference (%)	58,5	57,6	53,5	49,4	50,5	47,1	38,0

7.2 Drive Cycle Simulations

In this section some results from real drive cycle-based simulations are shown. First validation results are shown and then results of E-axle simulations are shown, which give good overall look of the performance and potential that the E-axle can provide based on these simulations. Comparisons between reference speed and simulated speed are shown for few results, but generally if the vehicle was able to follow the reference speed profile, the comparison won't be presented. Drive cycle-based simulations have some limitations due to the drive cycle matching the performance of the logged vehicle without E-axle, but with E-axle, the drive cycle will impose some limitations for the vehicle performance especially in up hills. Because of this, some simulations were run with modified speed profile, but with the same elevation profile in order to see better comparison between E-axle and ICE only vehicles.

7.2.1 Timber Truck Validations

Timber truck drive cycles consisted of varying speed and elevation profiles since it would drive different route almost every time. Load was not taken to same place every time and it was not picked up from the same place every time either. Also, timber truck mainly operates outside main highways which affects the speed and elevation profiles as well. Typical distances for unloaded (26t) and loaded (76t) drive cycles were around 100 km.

The simulated vehicle was validated by comparing simulated data with logged data. The GPS elevation data in timber truck was much more accurate on the move than in the other logged vehicles because the GPS device had sensor fusion with inertial sensors. The reference speed and elevation profile of the validation run for loaded timber truck is shown in Figure 32. Logged fuel during the drive cycle was 62,8 *l* and in simulation the fuel consumption was 58,2 *l*, thus simulation consumed approximately 7,3 % less fuel. The work done (energy) by engine in logged data was 262 kWh and in simulation it was 238 kWh, thus difference being 9,6 %.

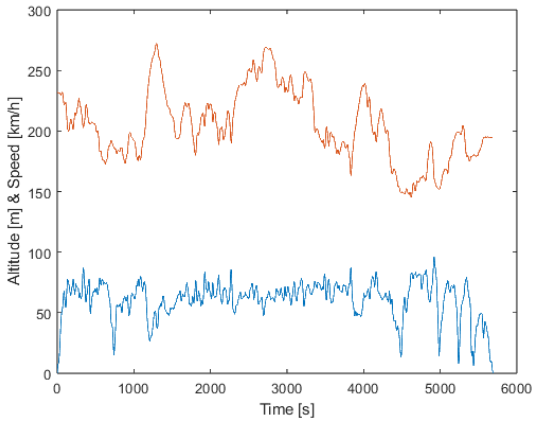

Figure 32. Drive cycle for loaded timber truck for distance of about 100 km.

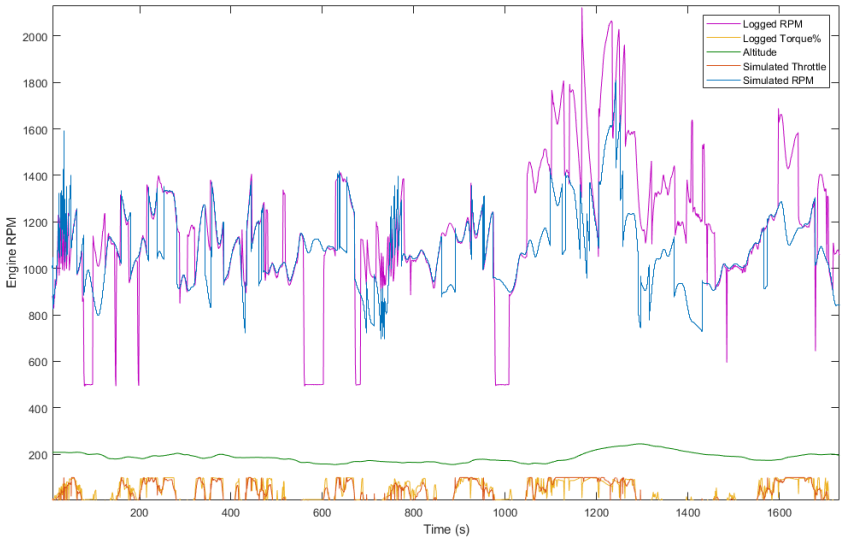

Figure 33. Comparison of logged and simulated data of loaded timber truck.

Comparison of logged and simulated data is shown in Figure 33, where it can be seen that the engine load values match each other very well indicating similar resisting forces between simulated and real vehicle. The engine rpm does not match equally well, which is due to the real vehicle obviously having much more sophisticated transmission control, which is predictive and also has different use modes. Comparison between reference speed and simulated speed during the validation run is shown in Figure 34. The difference in the engine speed and thus engine power may explain some of the difference between the simulated and logged engine work since the engine load matches well after all.

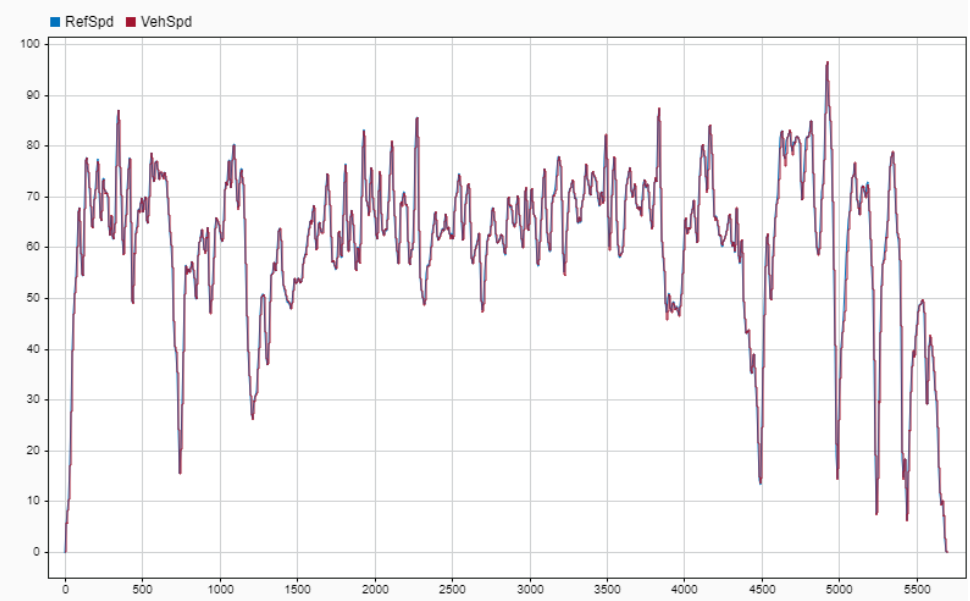

Figure 34. Comparison of reference speed and simulated speed for loaded timber truck validation run.

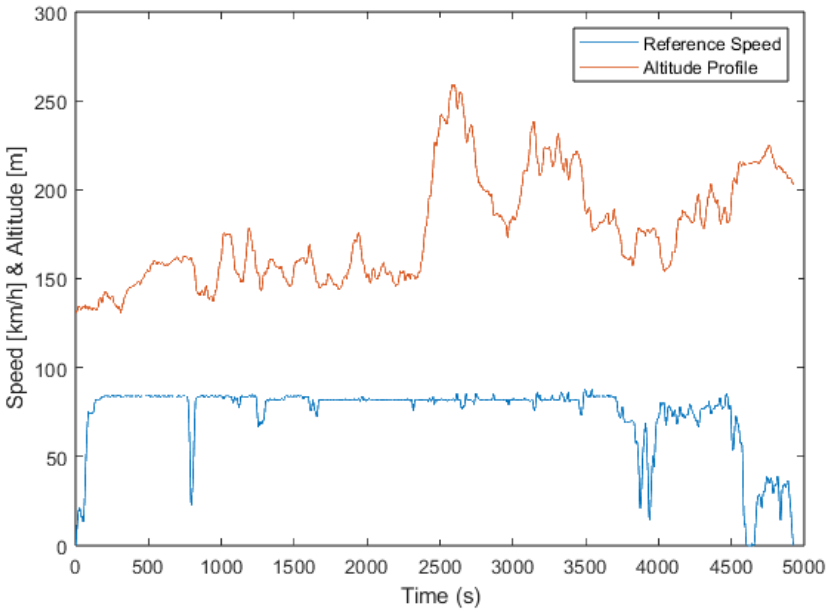

Figure 35. Drive cycle for unloaded timber truck. Distance approximately 102 km.

Validations run for unloaded (26t) timber truck was drive cycle that preceded the loaded drive cycle. So, the vehicle drove to loading site in the unloaded drive cycle and then left with a load to the unloading site in the loaded drive cycle. The drive cycle for the unloaded timber truck validation run is shown in Figure 35. The fuel used in simulation was 48 *l* and in logged data it was 40,7 *l*, thus difference being approximately 16,5 %. Energy used in simulation was 196 kWh and in logged data it was 194 kwh, thus difference being approximately 1 %. Clearly the efficiency of the simulated engine could have been better in partial load range.

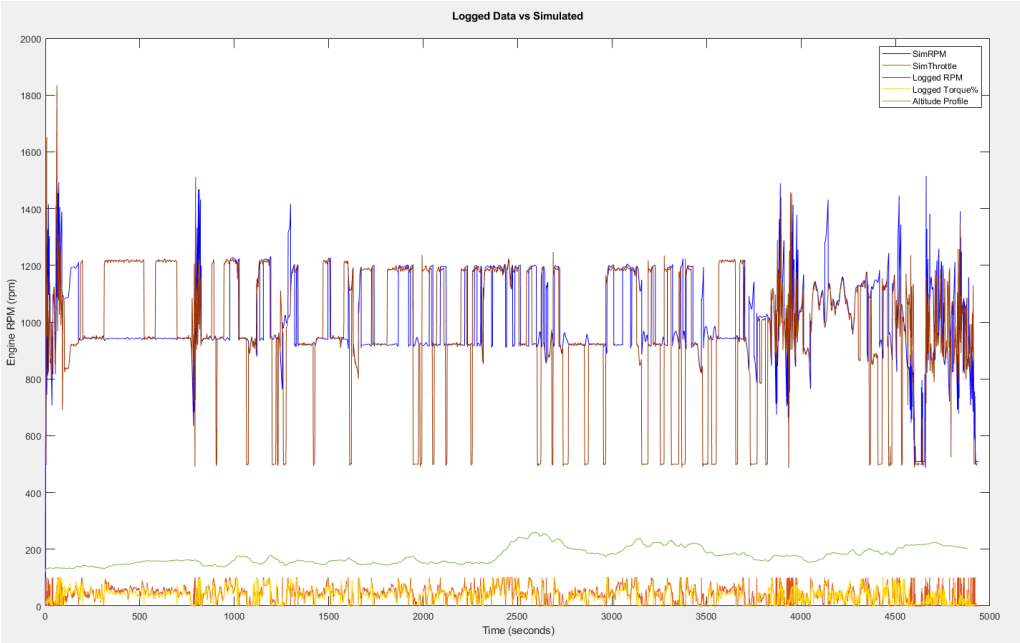

Figure 36. Comparison of simulated and logged data for unloaded timber truck.

Figure 36 shows the comparison between simulated and logged data for unloaded timber truck. The GCL seemed to work fairly well for unloaded vehicle, though at times the simulated and real vehicle use different gear. It is in the logic of the simulated vehicle to use high gear quite easily in down hills, whereas real vehicle easily free coasts down hills. Engine loads between simulated and real vehicle match very well, which is expected since the energy difference was so small. The simulated vehicle matched the reference speed profile perfectly in unloaded timber truck validation run.

7.2.2 Loaded Timber Truck with E-axle

The timber truck with E-axle was simulated with the logged speed profiles and with modified speed profiles, so that the logged speed profile would not restrict the movement of the vehicle in up hills for example when E-axle provides additional traction force for the vehicle. Results with modified speed profile as shown in Figure 37 are presented here, for R660 and R460. In the modified speed profile, most of the reference speed is set to constant 82 km/h, except for the beginning and the end of the cycle.

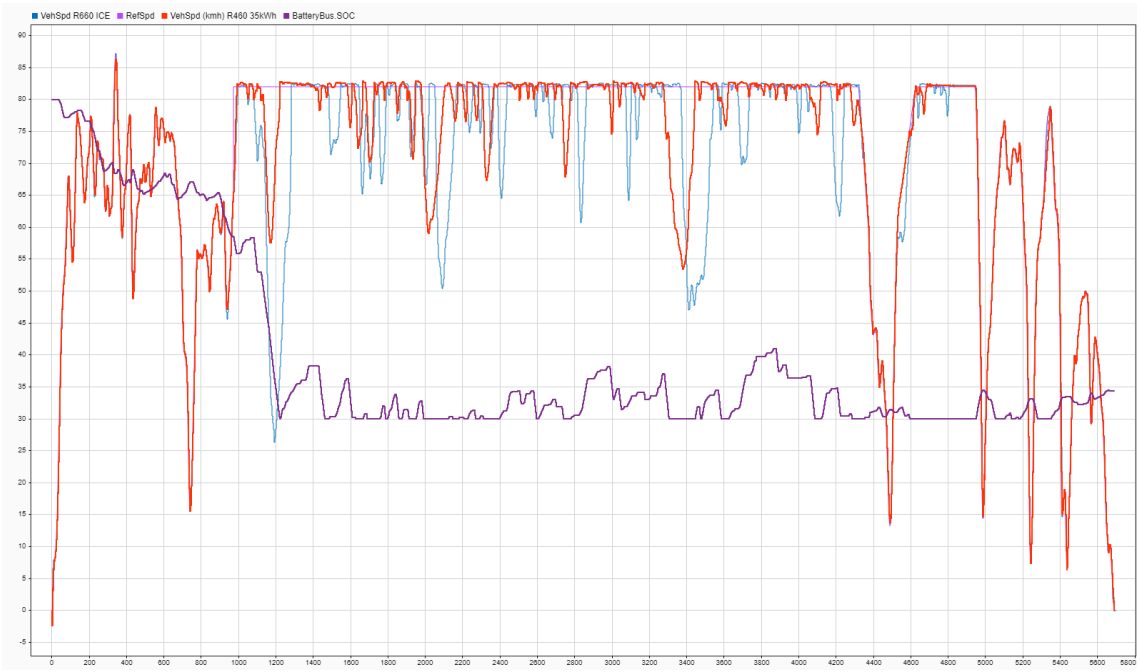

Figure 37. Modified speed profile for loaded timber truck R660 ICE vs R460 with E-axle.

The speed profile of the normal R660 (**blue**) was used as a baseline for the downgraded R460 with E-axle (**red**). The **purple** curve is battery SOC for 35kWh battery. The difference between R460 with E-axle and 35 kWh battery is shown in Figure 37, where it can be seen that the R460 with E-axle performs quite similarly or little bit better than R660 ICE only. At around 1200 s the difference in the total traction force between R660 and R460 is clearly shown since with the help of the E-axle, the speed of the R460 slows down a lot less in the hill compared to regular R660. With better E-axle control, the battery usage could be saved to the most challenging moments. Now, as can be seen in the beginning of the drive cycle, the battery energy is mostly used already in the beginning as the R460 is trying to follow the speed profile of a R660. In the middle section the difference in speeds cause the slowdowns caused by hills to happen at slightly different times since the vehicles arrive to the hills at different times. However, in overall it can be seen that in hills when there is battery energy, the R460 is able to perform slightly better or around the same as R660.

In all of the following figures, results with different battery sizes are shown so that **20 kWh has green**, **35 kWh has red,** and **50 kWh has blue** curve, for fuel and battery SOC.

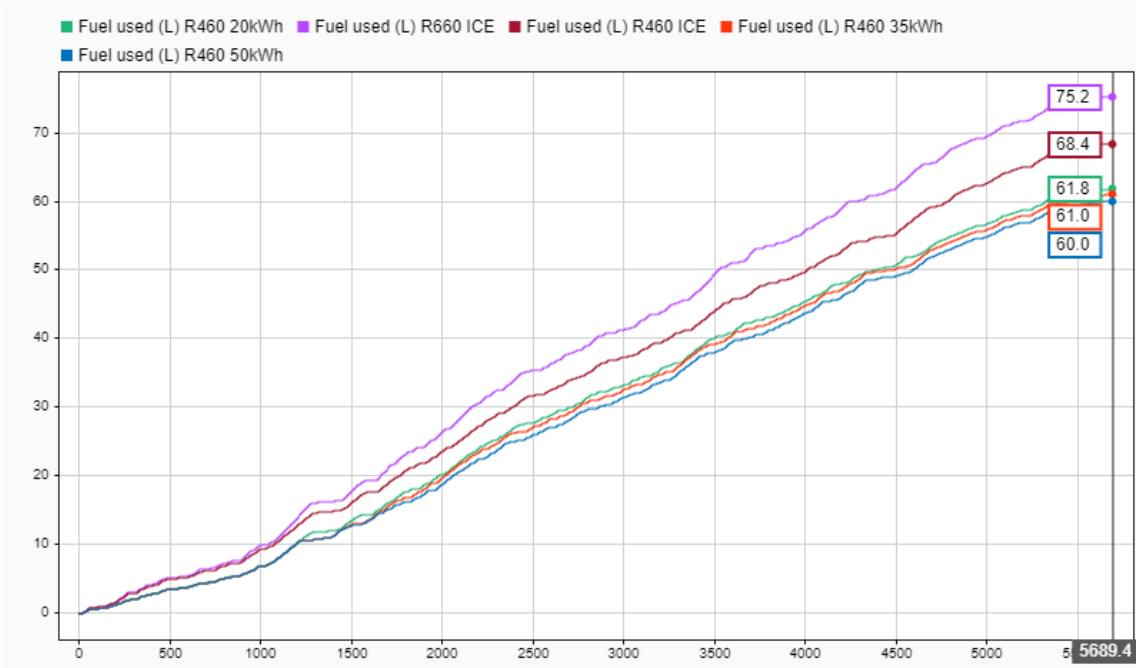

Figure 38. Fuel used between R460 E-axle and R660 ICE.

Even though the peak efficiency of the R460 was approximately 41 % in the simulation and the peak efficiency of the R660 was approximately 45 %, the R460 ICE still provided 9 % less fuel consumption compared to R660, but of course, the overall power of the R460 ICE is not sufficient for 76t combination. When E-axle was added to the R460, the consumption decreased further by 9,6 % – 12,3 % as seen in Figure 38.

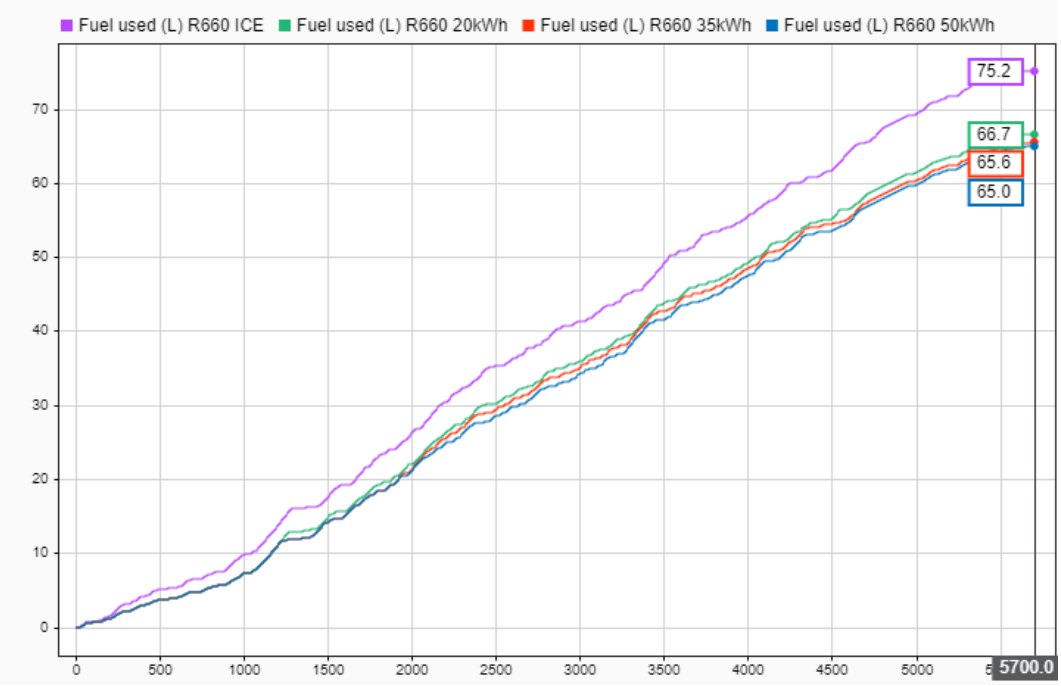

Figure 39. Fuel used between R660 ICE and R660 E-axle.

The fuel consumption of R660 with and without E-axle is shown in Figure 39. The decrease in consumption between R660 ICE and R660 HEV with 20 kWh battery is approximately 11,3 %. For R540 the decrease in percentage was approximately the same as for R660 with E-axle. Similar results circling around 10 – 20 % decrease in consumption were seen throughout timber truck drive cycles. Finally, battery SOC is shown for R460 and R660 with E-axle in Figure 40 and Figure 41 respectively, where **green is for 20 kWh, red is for 35 kWh and blue is for 50 kWh battery**. These three figures represent the effect of control logic for the E-axle very well. Both figures look almost the same when compared to each other. The most influential factor is the engine of the vehicle, determining its overall operational capability and thus determining the amount of E-axle used. Thus, fuel consumption reduction seen here, could be even better with better control logic, if everything else remains the same.

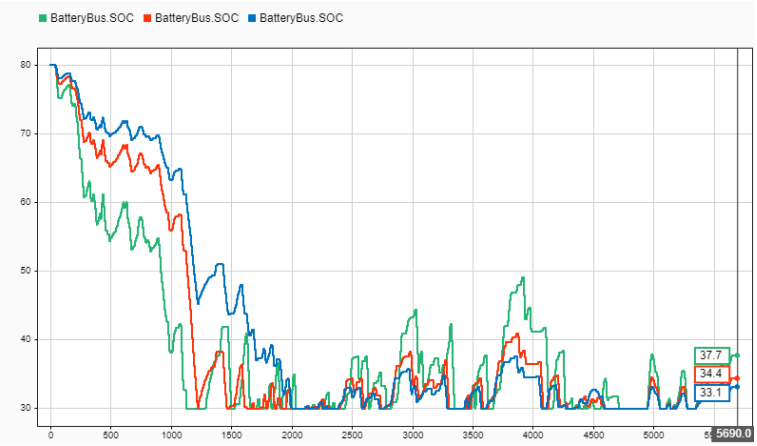

Figure 40. Battery SOC for R460 with E-axle.

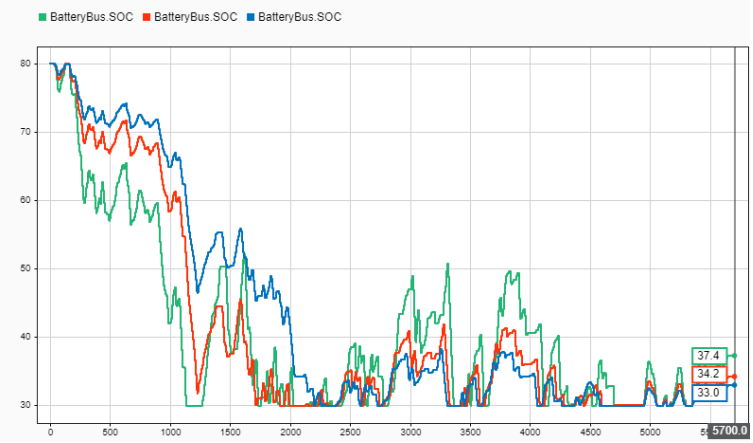

Figure 41. Battery SOC for R660 with E-axle.

7.2.3 Unloaded Timber Truck with E-axle

Results for unloaded timber truck with E-axle are presented here with the same drive cycle that was used in the validation run (Figure 35). The battery was empty at the beginning of the simulation, in order to see regeneration potential and the effect on fuel consumption. It is especially important for timber truck to be able to regenerate enough energy during normal driving operations since timber trucks often operate around the clock and also in such areas that charging from mains electricity would not be possible. Results for fuel consumption and battery SOC for R660 are presented in Figure 42.

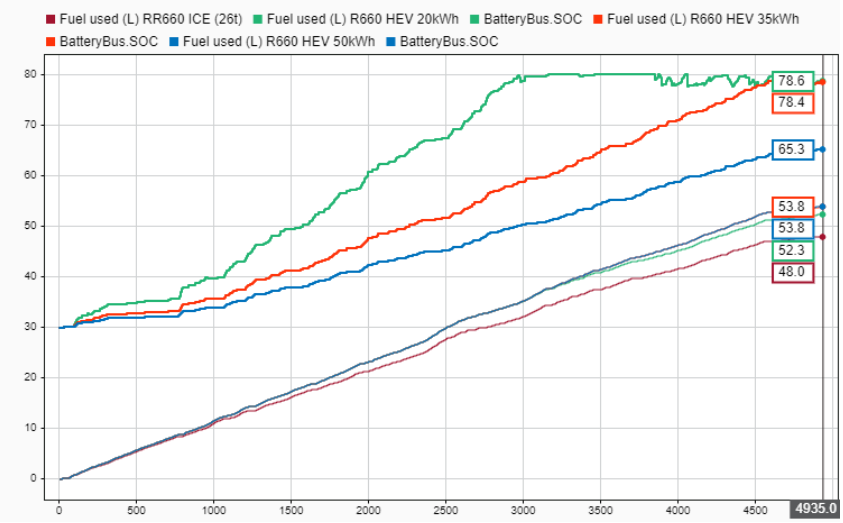

Figure 42. Fuel consumption and battery SOC for R660 during regeneration driving.

The increase in consumption with R660 E-axle compared to ICE only with 20kWh battery was 9 %. With 35 kWh and 50 kWh batteries, the results ended up being exactly the same with increase of 12,1 %, meaning that the control strategy should have been more aggressive or otherwise better made. Though, with more aggressive control logic, the increase in consumption for 35kWh and 50 kWh batteries would have been even greater. Also, it can be seen that with 20 kWh battery, the battery gets full well before the end of the drive cycle, meaning that with better control, the regeneration rate could be optimized so that the battery gets full a little bit before the end.

When fuel consumption results from driving unloaded and loaded ICE powered vehicle was compared with the same results from E-axle assisted model, the total achievable net fuel savings were on average around 6 %. This depends between drive cycles so that negative net effects are also possible with the model and control logic used.

7.2.4 Long-haul Truck ICE

Long-haul truck drive cycle consisted of mostly constant speed driving on highway with minimal amounts of stop and goes or accelerations and decelerations. The truck was operating on the same route for the time it was logged, and the distance was approximately 340 km. Profile of the one drive cycle for long-haul truck is shown in Figure 43. Since the driven route for the long-haul truck was the same throughout logging, all the drive cycle profiles were very much identical as well.

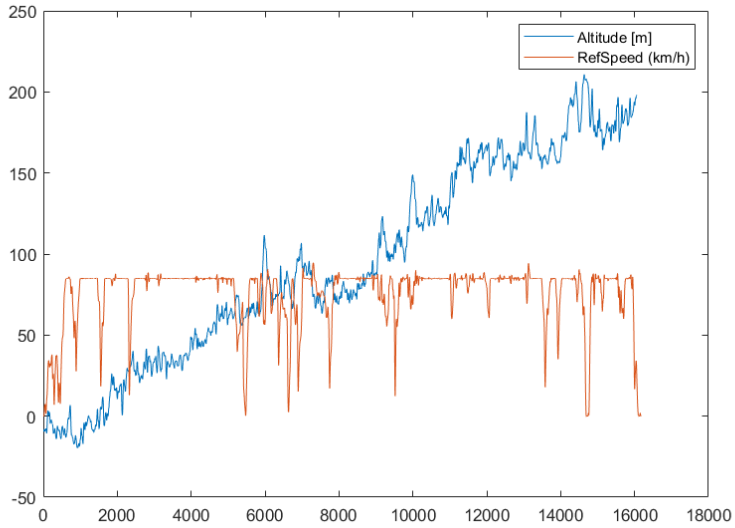

Figure 43. Drive cycle for loaded long-haul truck for distance of 338 km.

The simulated vehicle was validated similarly to timber truck by comparing simulated data with logged data, so that the simulated vehicle would drive logged drive cycle with logged elevation and reference speed profile. However, the GPS elevation data with long-haul truck proved to be quite difficult to work with, since the GPS in the logging device had no inertial sensors, which would allow sensor fusion between GPS data and inertial sensor data to offer better accuracy in elevation.

Engine work and fuel consumption were measured for validations run and compared. For the long-haul truck validation, the engine work was 863 kWh in logged data and 820 kWh in simulated data, thus difference being approximately 5,1 %. However, fuel consumption was 199,7 *l* in simulation and 189 *l* in logged data, thus simulation consumed 5,7 % more fuel.

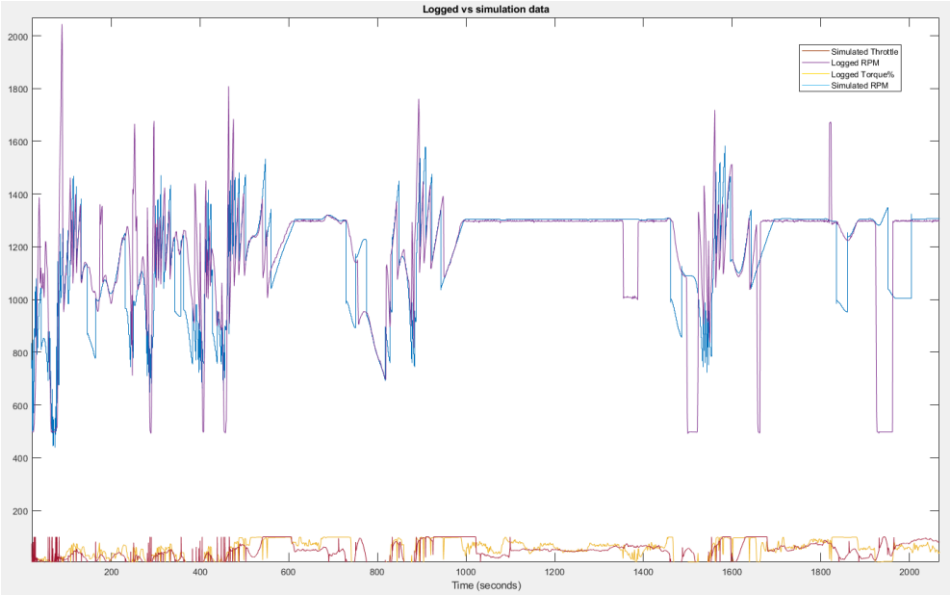

Figure 44. Logged vs simulated long-haul data.

In Figure 44, simulated and logged data are compared. It can be seen that the engine speed, and thus vehicle speed matches reasonably well (upper curve), also gear changes match between logged and simulated data reasonably well. The logged engine load vs simulated engine load (throttle position) does not seem to match equally well but at the same time the energy difference was only 5,1 %. Since the difference between engine energies (work done) was relatively close and within 10 % difference, the simulation was deemed accurate enough for concept level study. The difference between simulated vehicle speed and reference speed for long-haul validation is shown in Figure 45.

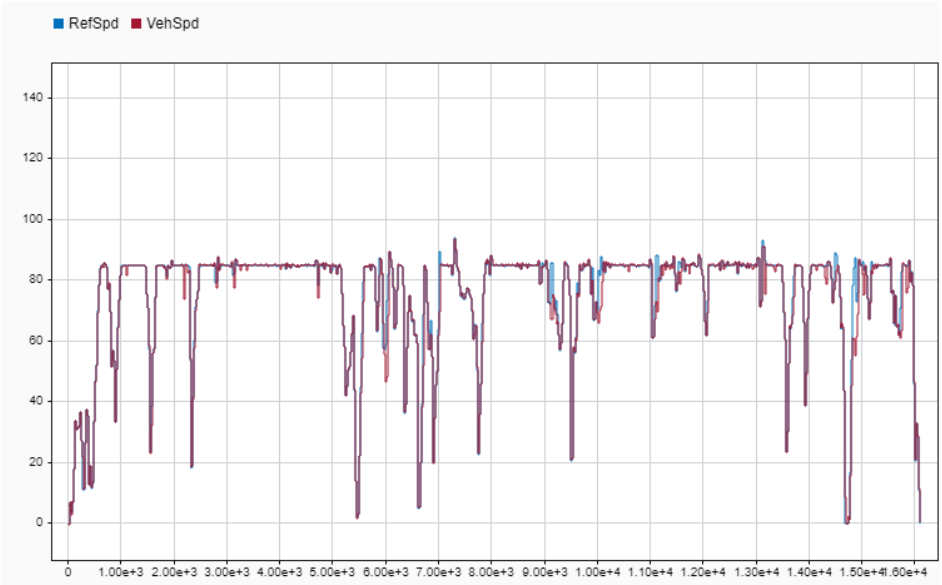

Figure 45. Difference between reference speed and simulated speed in loaded long-haul cycle.

Validations run for unloaded (24t) long-haul truck was same route as loaded run but driven to other direction. Reference speed and elevation profile are shown in Figure 46.

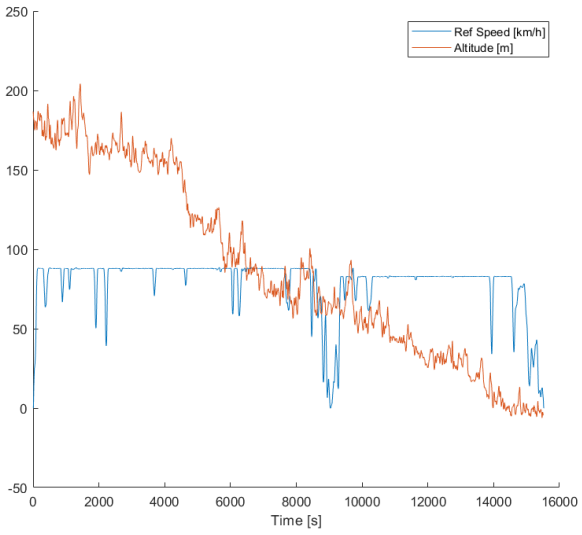

Figure 46. Reference speed and elevation profile for unloaded long-haul truck.

Driven distance was same as for loaded drive cycle. The fuel used in simulation for unloaded long-haul truck was 118,4 *l* and in logged data it was 98,5 *l*, thus simulation

consumed 20,2 % more fuel. Energy usage at the engine was 468 kWh in simulation and 463 kwh in logged data. Difference being approximately 1 %. The fuel consumption number quite clearly indicate that the overall efficiency of the simulated engine was too low. The elevation profile for the long-haul truck for both directions is basically elevation change from coastline to inner continent even though it seems like constant up or down hill. The long distance makes the natural elevation change between inner continent and coastline visible.

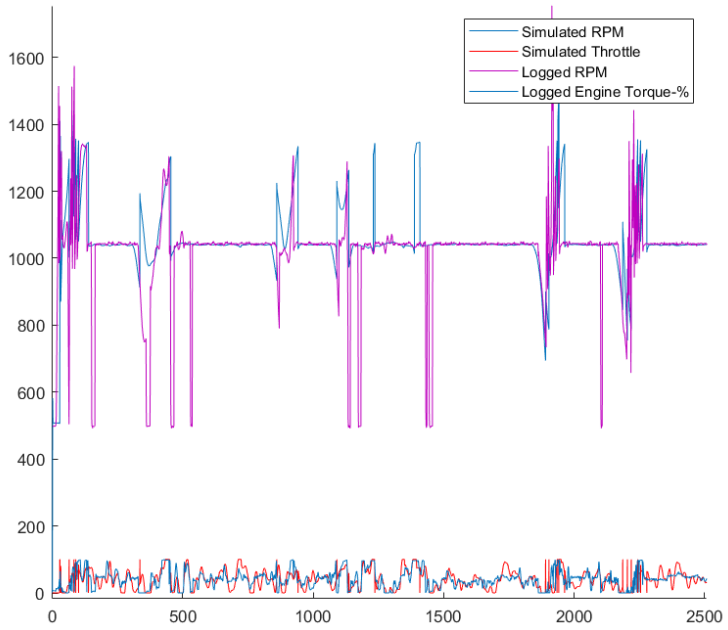

Figure 47. Simulated vs logged data for unloaded long-haul truck.

The simulated and logged data for unloaded long-haul truck are shown in Figure 47, where it can be seen that engine rpm and gear changes match reasonably well. Again, much more fluctuation is between the simulated and logged engine load.

7.2.5 Loaded Long-haul Truck with E-axle

After validations the vehicle was simulated with E-axle both loaded and unloaded. In loaded drive cycle the battery was full in the beginning and in the unloaded simulations battery was empty. Fuel consumption savings between approximately 5–9 % were seen with loaded R540 long-haul drive cycle with nominal battery sizes between 20–50 kWh,

as shown in Figure 48. Similarly to previous results with timber truck, **green represents 20 kWh results, red represents 35 kWh results, and blue represents 50 kWh results.**

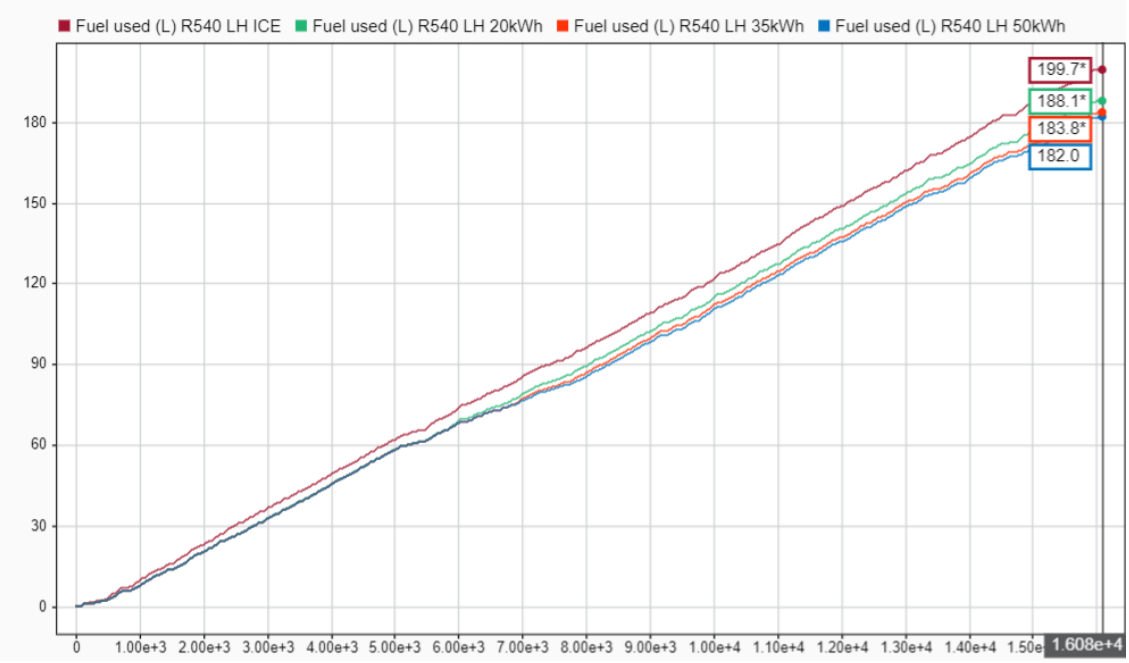

Figure 48. Loaded long-haul truck fuel consumption with E-axle.

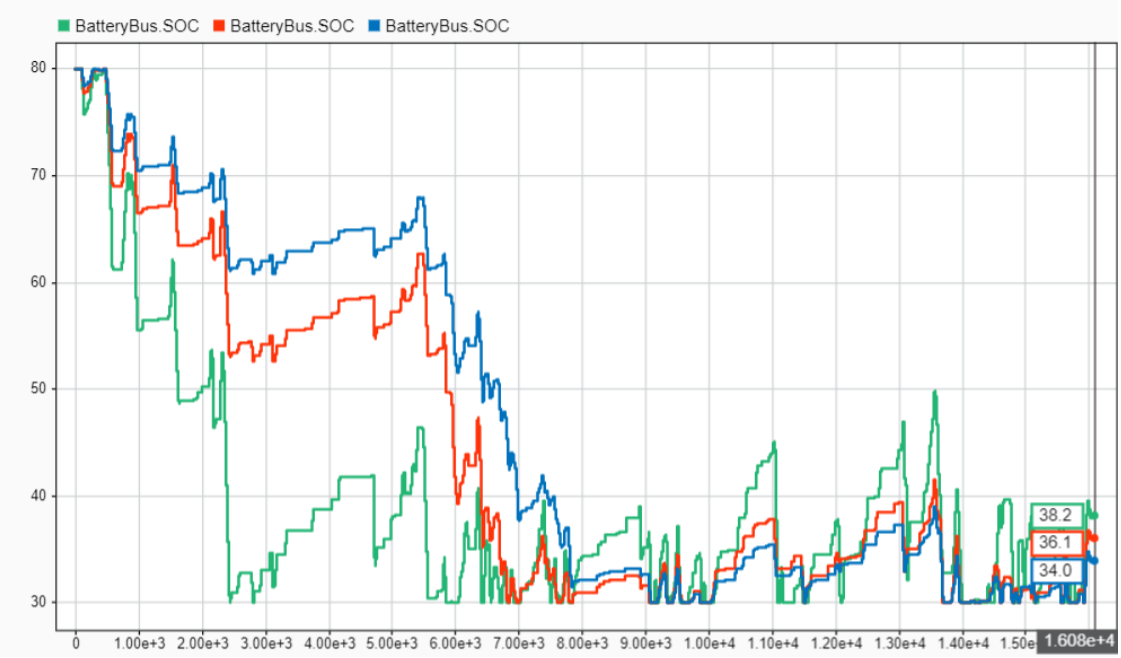

Figure 49. Battery SOC for 20 kWh (green), 35 kWh (red) and 50 kWh (blue) batteries. for long-gaul truck.

In Figure 49 battery state of charge is shown for different battery sizes. The lack for predictive E-axle control is easily seen in Figure 49, so that each battery size follows exactly the same pattern. It can also be noticed that fuel reduction potential seems lower with long-haul cycle than it does for example with timber truck drive cycle. The fact that most of the driving consists of constant speed driving, means that the fuel saving potential must also come from that. If on the other hand, drive cycle consists of many decelerations and accelerations, the potential for the E-axle is higher as more energy can be recuperated and the E-axle boosted accelerations are greater portion of the drive cycle. In constant driving the E-axle is not used as much, and if it were to be used, the electrical energy and hence battery size would have to be a lot greater. Then recuperated potential would decrease, and the need for charging from mains electricity would increase, which would mean different working cycles for the vehicle and completely different usability for the E-axle. When long-haul truck was simulated with the same drive cycle with timber truck, similar fuel reduction values were observable as for timber truck.

The long-haul truck was also simulated with 460 hp engine and the fuel consumption values in the same test for R460 with E-axle are shown in Figure 50, where it can be seen that the consumption savings with E-axle were approximately between 4–6 %. With any battery size, the R460 with E-axle followed the reference speed profile very much like R540 ICE.

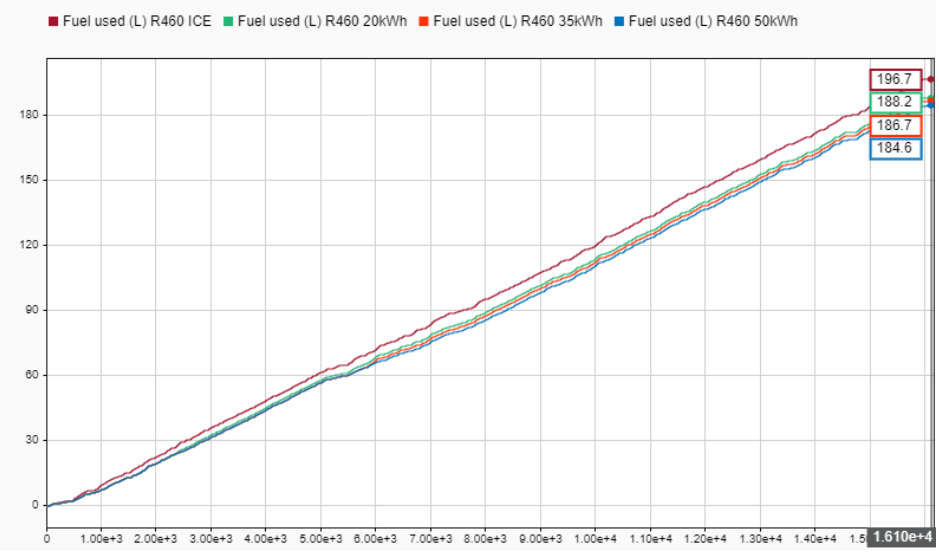

Figure 50. Fuel consumption values for loaded R460 with E-axle.

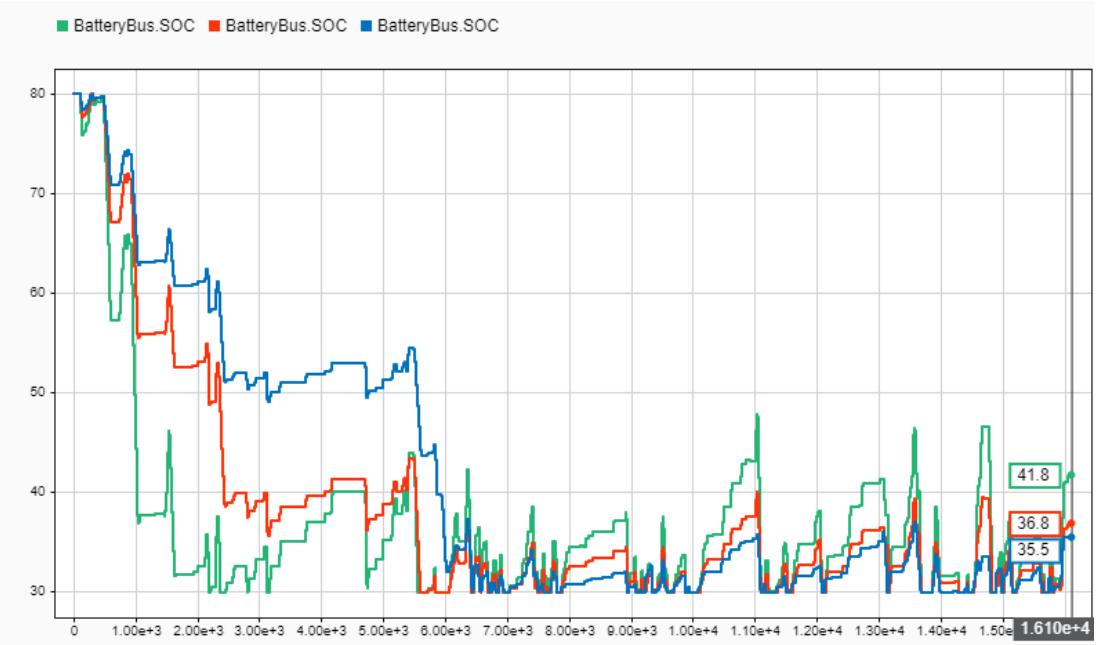

Figure 51. Battery SOC for loaded R460 with E-axle.

Battery SOC for R460 is shown in Figure 51, where it can be seen that the battery usage is higher for R460, but follows the pattern of the R540, which is expected.

7.2.6 Unloaded Long-haul Truck with E-axle

Previously shown unloaded drive cycle was simulated with E-axle, so that the battery was empty in the beginning. With R540 the fuel consumption increase was approximately between 2 – 5 %, as can be seen in Figure 52.

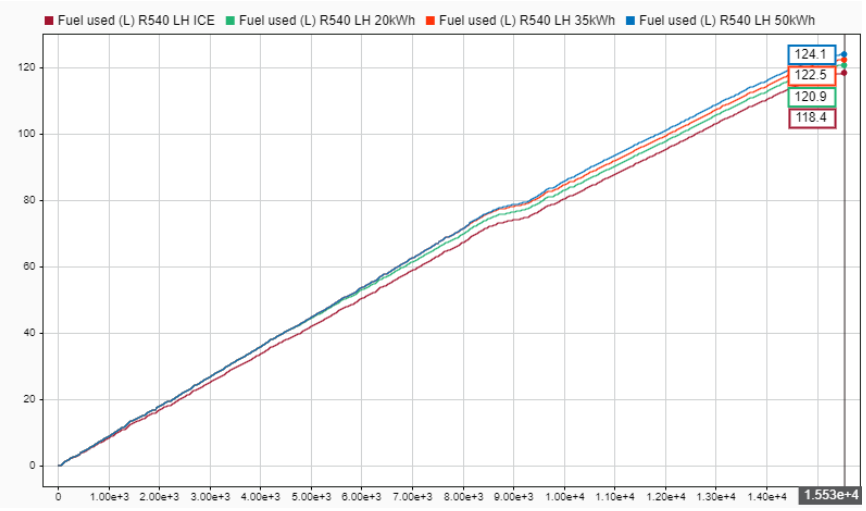

Figure 52. Fuel consumption with unloaded R540 with E-axle.

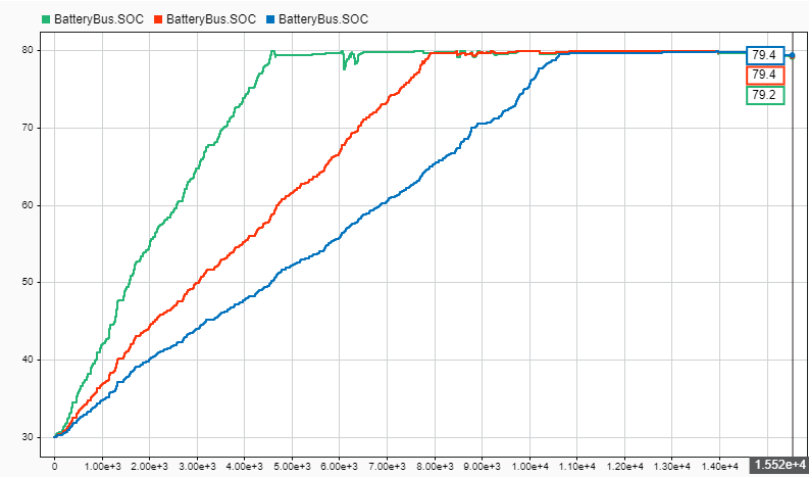

Figure 53. Battery SOC for unloaded R540 long-haul truck.

The battery SOC for this drive cycle is shown in Figure 53 and since the drive cycle was so long, every battery size got full. With long driving distance the charging power can also be lower so that charging of the battery can be better divided throughout the drive cycle. With short drive cycles the charging power has to be higher if all the energy is to be generated by driving operations. Fuel consumption and SOC for R460 long-haul are shown in Figure 54. For R460 the fuel consumption increase for regeneration driving was approximately between 3,0–6,5 %.

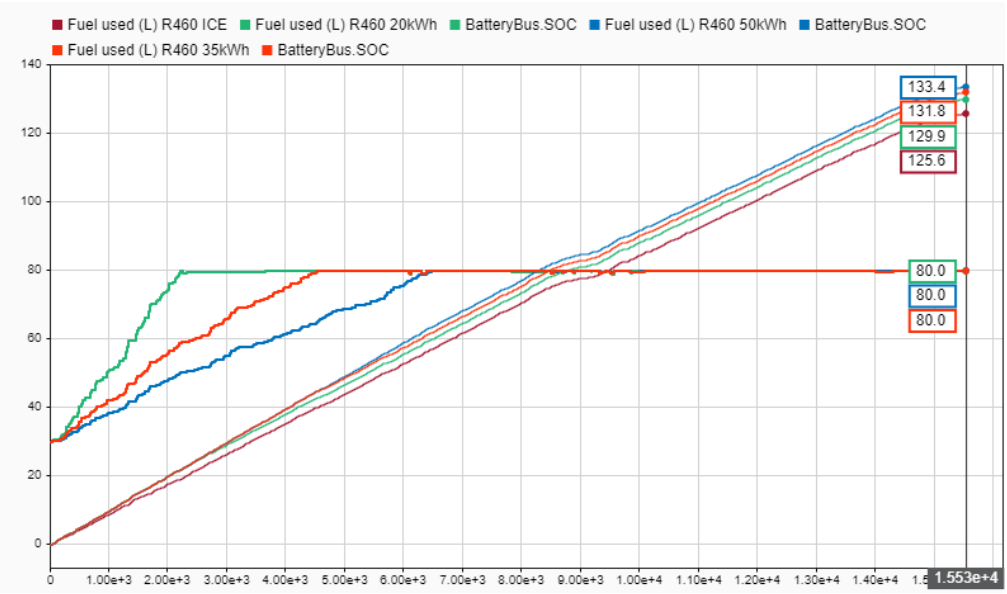

Figure 54. Fuel consumption and SOC for unloaded R460 long-haul.

Interestingly though, the R460 seems to get the batteries full much earlier than R540. Most likely the MCL parameters have changed at some point, which causes the behavior, since with same logic as for R540, the charging should take longer for the R460. No other apparent reason could be found for this. This difference; however, is not crucial, but only demonstrates the importance of the control logic for the functionality of the E-axle. The unloaded R460 followed the reference speed profile perfectly.

7.2.7 Tipper Truck Validations

Validation for tipper Truck was done similarly to long-haul and timber truck. The used drive cycle speed and elevation profile for validation is shown in Figure 55. Similarly, to long-haul truck, the elevation profile looks like strong downhill, but is just elevation change from inner continent to coastline. Fuel used in simulation was 40,7 *l* and in logged data it was 45,9 L, thus simulation consumed approximately 11,3 % less fuel. Engine work done in simulation was 164 kWh and in logged data it was 169 kWh, thus difference being approximately 3 %. Driven distance in this drive cycle was approximately 70 km. The driven distances for tipper truck drive cycles were ranging from just couple of kilometers, up to about 100 km.

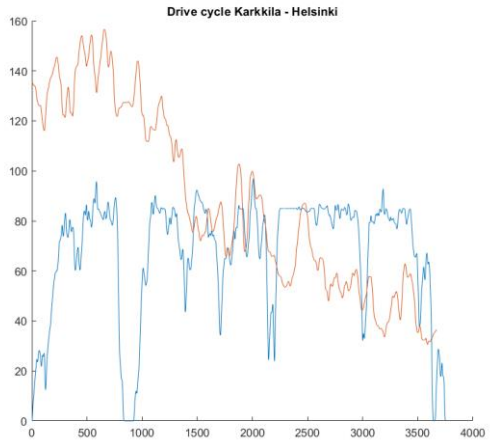

Figure 55. Drive cycle profile for loaded tipper truck.

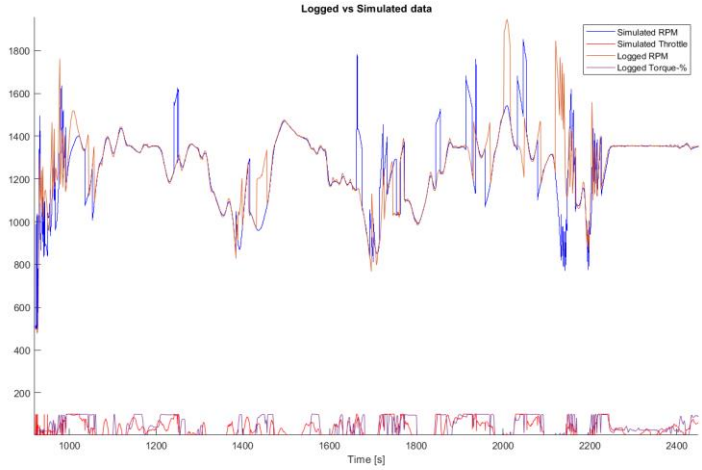

Figure 56. Comparison of logged and simulated for loaded tipper truck.

Comparison between logged and simulated data is shown in Figure 56. It can be noticed that the there is one point when retarder was used around 2100 s, which was not simulated. Also, it can be seen that, the simulated vehicle will change to lower gear more easily in up hills than the real vehicle did. This is the same behavior caused by the GCL, which has been observed with every simulated vehicle. Engine load between logged and simulated data do not match as well as could be expected by the result, however, the simulated value follows the logged value reasonably well. Error may occur from the imported data in MATLAB, as well as from the GPS-based elevation profile. Reference speed and simulated speed matched very well, with only minor difference, as shown in Figure 57.

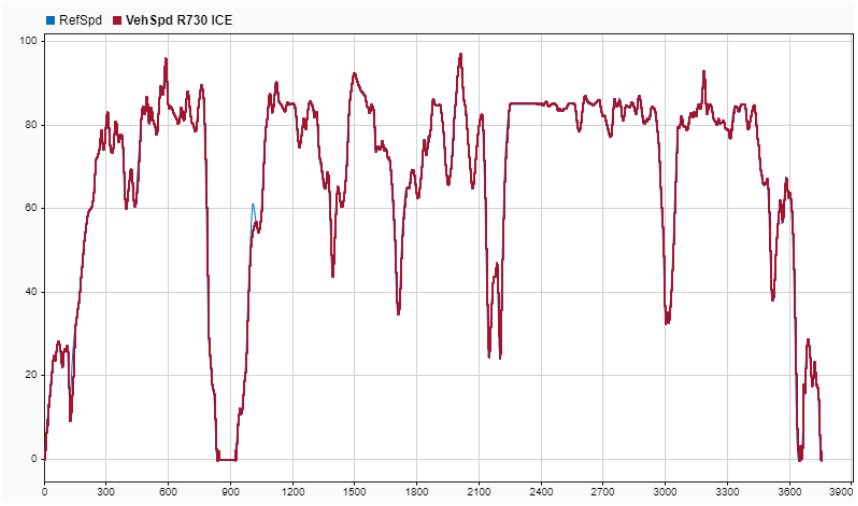

Figure 57. Tipper truck reference speed vs simulated speed.

With unloaded tipper truck the validation drive cycle was as shown in Figure 58, with driven distance of approximately 74 km. Fuel used in simulation for unloaded tipper truck was 32,9 *l* and in logged data it was 31,4 *l*, thus simulation consumed approximately 4,8 % more fuel. Engine energy in simulation was 129 kWh, but in logged data it was 140 kWh, thus difference being approximately 8,2 %.

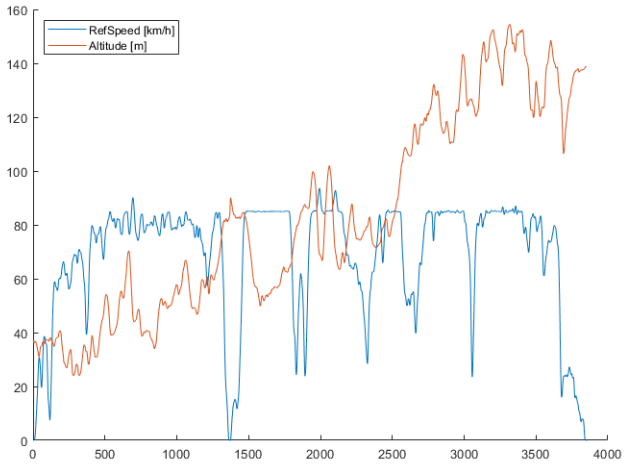

Figure 58. Drive cycle profile for unloaded tipper truck.

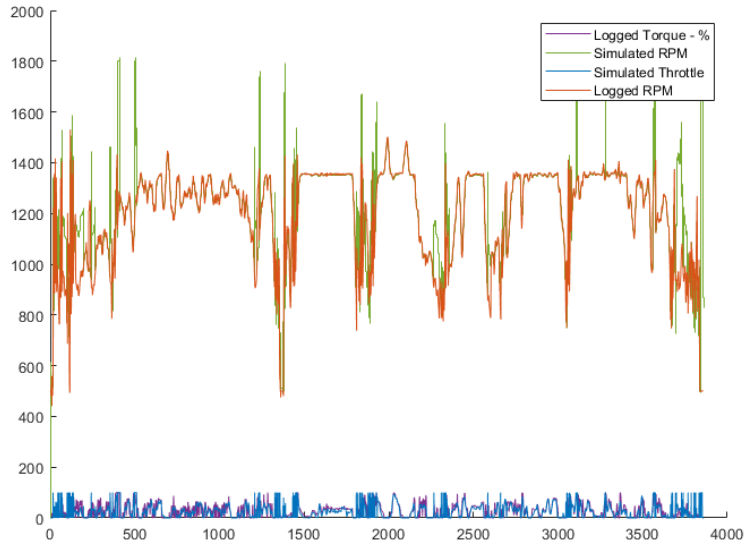

Figure 59. Logged vs simulated data for unloaded tipper truck.

The simulated data and logged data match reasonably well, as seen in Figure 59, even though the energy difference was 8,2 %. It can also be seen that the simulated vehicle tends to change for lower gear more easily in up hills than the logged vehicle did. The reference speed and simulated speed matched also very well, as can be seen in Figure 60.

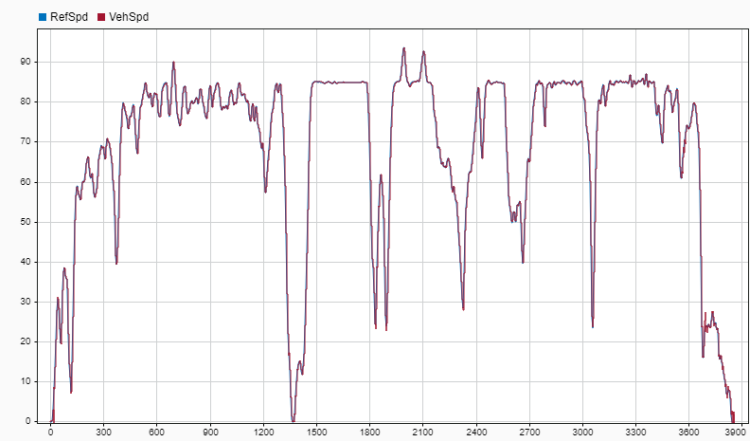

Figure 60. Comparison of reference speed and simulated speed for unloaded tipper truck.

7.2.8 Loaded Tipper Truck with E-axle

After validations the vehicle was simulated with E-axle both loaded and unloaded. In loaded drive cycle the battery was full in the beginning and in the unloaded simulations the battery was empty just like in the case of long-haul and timber trucks. In overall, fuel consumption savings of approximately 10–20 % were seen with loaded tipper truck drive cycles with battery sizes between 20–50 kWh. The vehicle was simulated with the regular 730 hp engine with E-axle and then with 540 hp with E-axle. Couple of results are shown here.

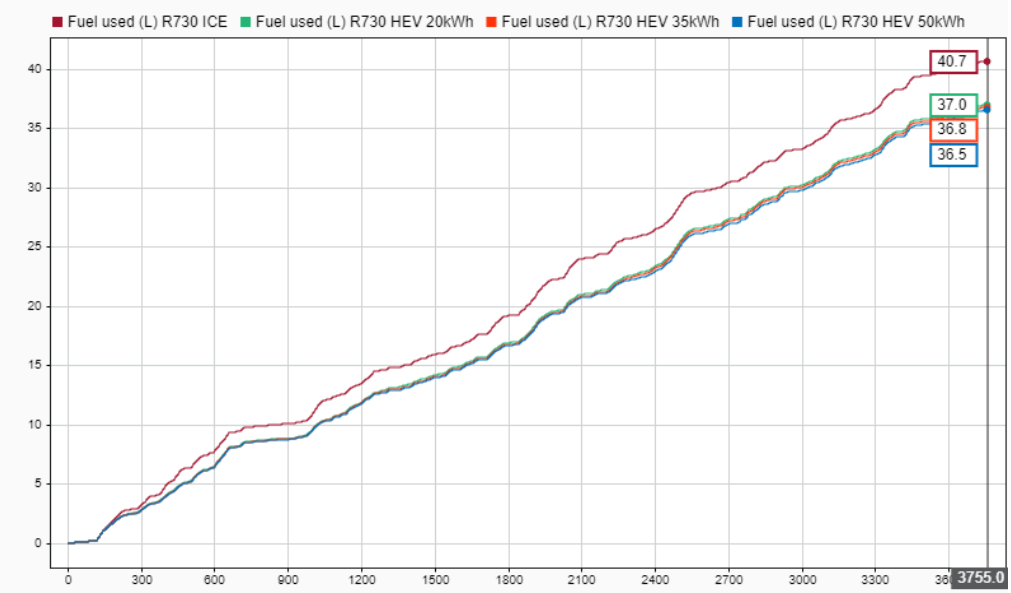

Figure 61. Fuel consumption between R730 ICE and R730 HEV.

The difference in fuel consumption between loaded R730 with and without E-axle in the same drive cycle as in validation is shown in Figure 61. With E-axle and 20 kWh battery, the reduction in fuel consumption was 9 %, and with 50 kWh the reduction was 10,3 %. The reduction value between the largest and smallest battery suggests that the control logic would have to be better. In general, it was tested that, with the used control logic but different control parameters, it is possible to see reduction of at least up to 11 % with the 20-kWh battery. However, all the results shown here are with the same control logic parameters, as mentioned in the section 5.4 of this thesis, in order to keep the number of variables in reasonable levels.

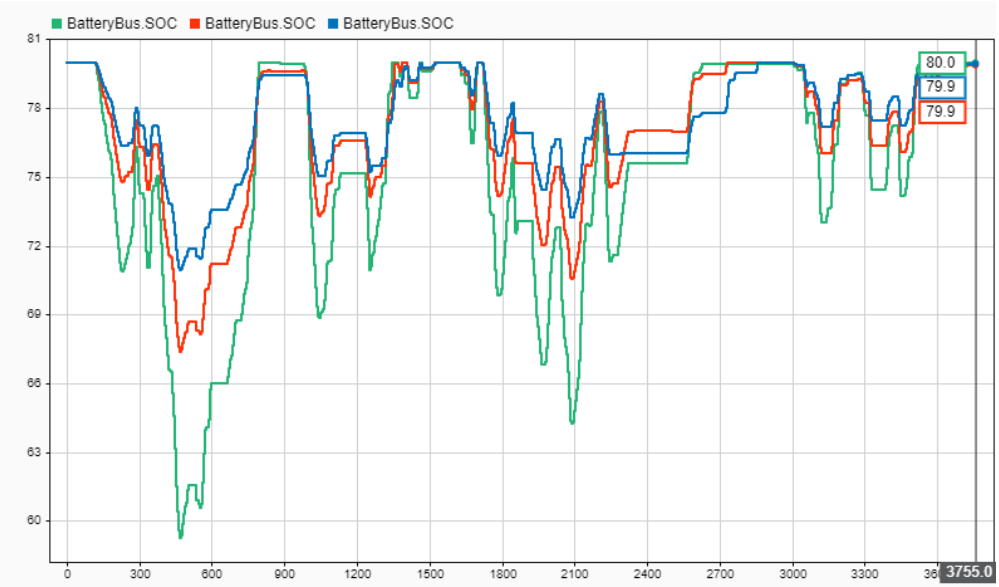

Figure 62. SOC for loaded tipper truck with E-axle.

The corresponding battery SOC for the different batteries in the same drive cycle are shown in Figure 62. Interestingly enough, this was the only drive cycle between each tested vehicle, during which the battery got back to full at the end of the drive cycle without any algorithm designed to do that. However, as can be seen, the usage of the battery energy was not very high in this drive cycle. At lowest the battery SOC went to 60 % when the lowest allowed was 30 %. This is most likely due to the control parameters for the E-axle boosting being too low for the R730, but also because of the drive cycle profile.

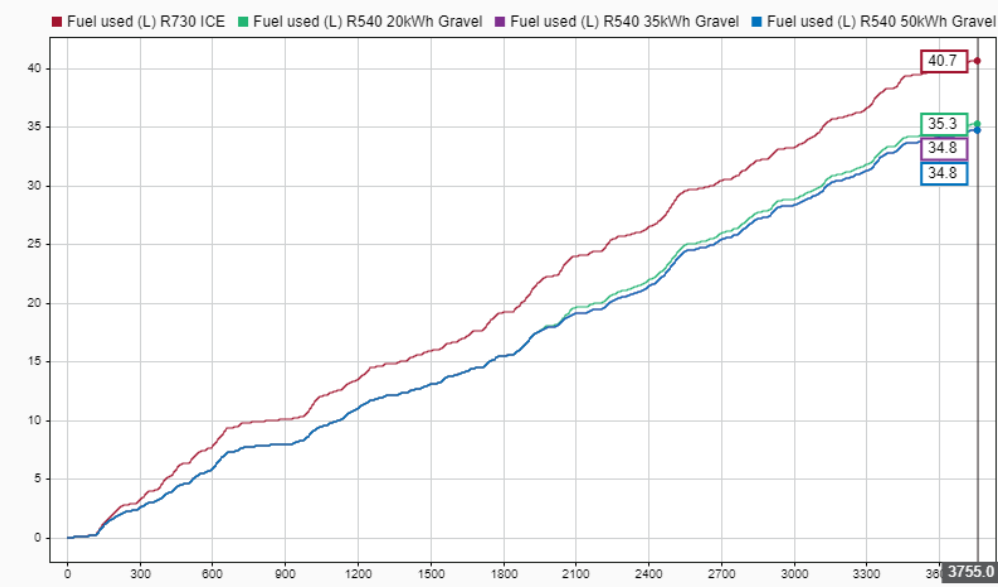

Figure 63. Fuel consumption of R540 tipper truck with E-axle.

After R730, the same drive cycle was tested with R540 tipper truck with E-axle. The fuel consumption results are shown in Figure 63, where it can be seen that compared to R730 ICE, the R540 with 20 kWh battery can reduce fuel consumption by 13,3 % and with 35-kWh battery the reduction is 14,5 %. With 50 kWh battery there is no more reduction because not all battery energy was used, so 35 kWh and 50 kWh batteries naturally achieved the same performance with the same control logic. However, unlike in the case of R730, the battery levels did not reach back to 80 % with R540, as can be seen in Figure 64, because with smaller engine more of the E-axle is used.

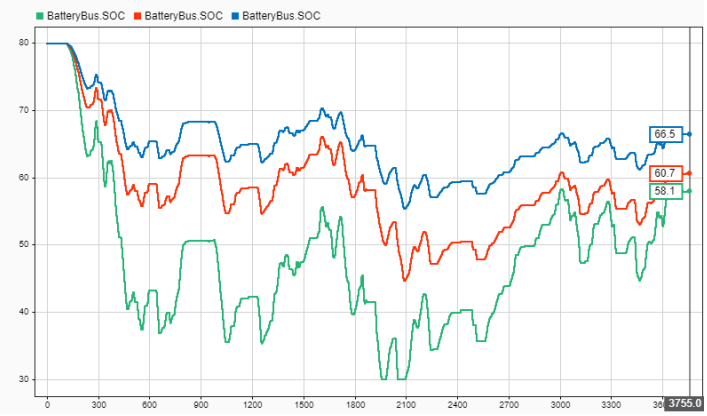

Figure 64. Battery SOC with loaded R540 tipper truck.

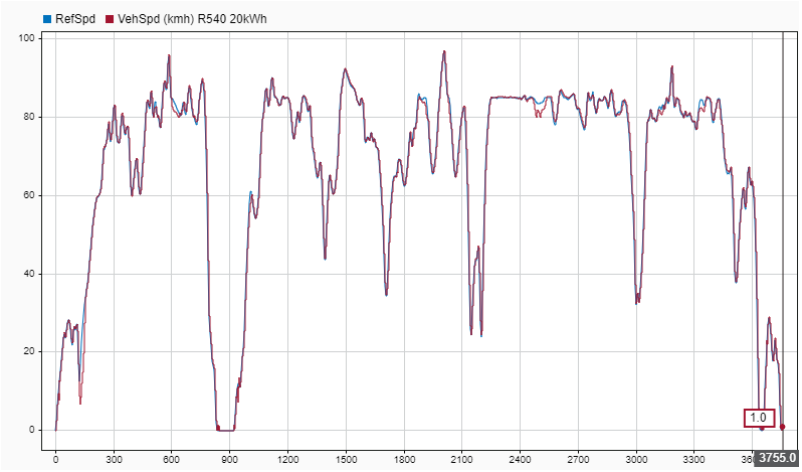

Figure 65. Reference speed vs simulated speed for R540 E-axle.

The speed profile with R540 and 20 kWh battery is shown in Figure 65, where it can be seen that the R540 with E-axle is able to achieve functional performance comparable to the R730 ICE.

7.2.9 Unloaded Tipper Truck with E-axle

Previously shown unloaded drive cycle for the tipper truck was used to determine fuel consumption for regeneration driving with empty R730 tipper truck. Fuel consumption increase with 20 kWh battery was 16,4 % as shown in Figure 66. With 50 kWh battery the increase was 22,4 %. The 20 kWh battery got full about halfway of the drive cycle, while for 35 kWh battery it took almost whole drive cycle to reach a full battery and with 50 kWh battery the battery reached only 70,8 % of total 80 %. Basically, the 35 kWh battery was the most optimized in terms of time when the battery got full. 50 kWh battery would have needed different control logic to reach full level.

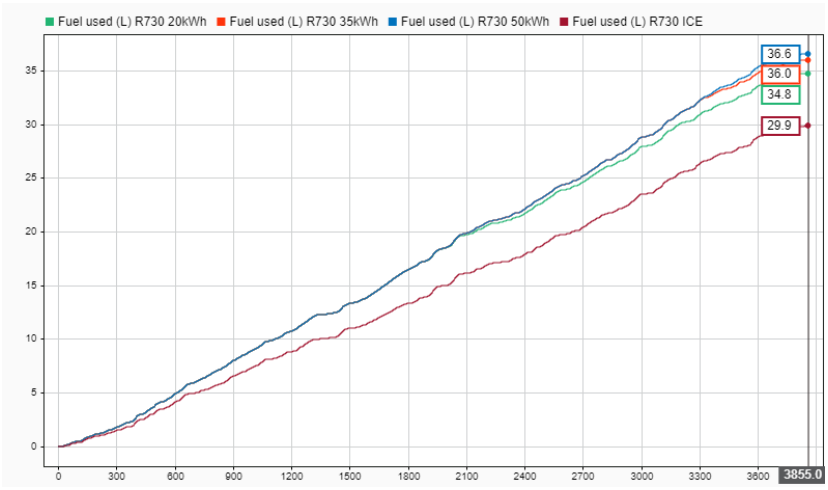

Figure 66. Fuel consumption for unloaded R730 tipper truck with and without E-axle.

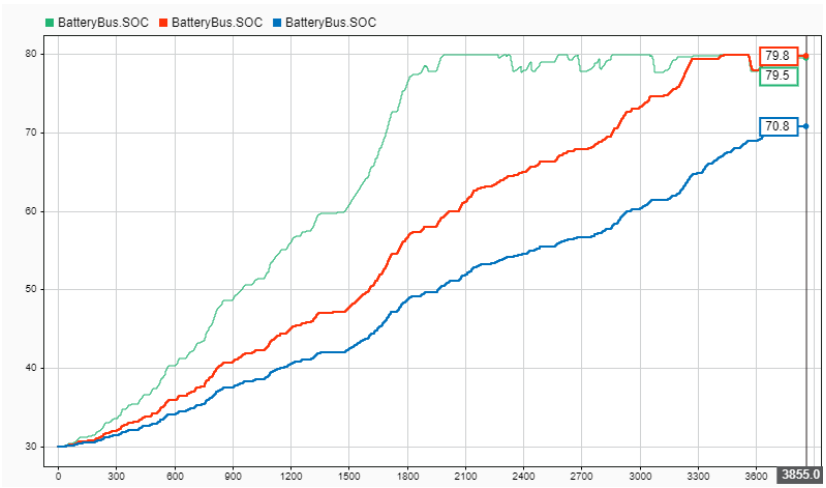

Figure 67. Battery SOC for unloaded tipper truck.

With R540 tipper truck with E-axle, the fuel consumption increase with 20 kWh battery was 13,7 % and for 35 kWh battery the increase was 17 % as shown in Figure 68. Once again since the control logic was the same, 50 kWh battery did not reach full level, but instead performed the same as 35 kWh battery. This can be seen in Figure 69. Compared to R730, the increase in consumption was lower and it took longer time to get the batteries full. The net fuel consumption savings for tipper truck with E-axle were around -1 – 5 % and the saved braking energy for the gravel truck drive cycles were around 30 – 45 %.

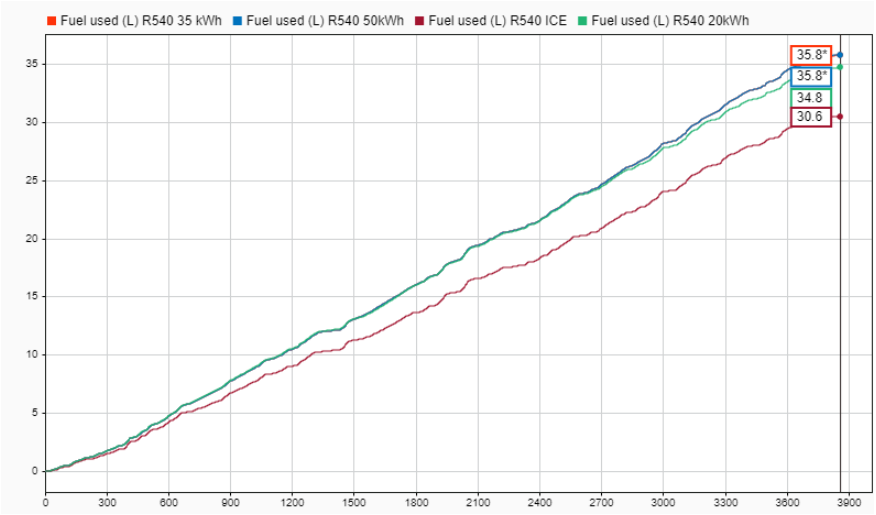

Figure 68. Fuel consumption for unloaded R540 tipper truck with and without E-axle.

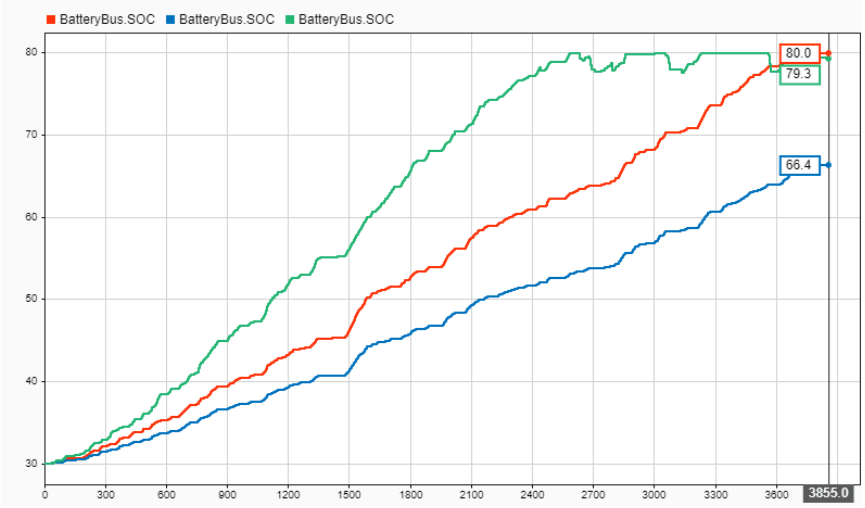

Figure 69. Battery SOC for unloaded R540 tipper truck.

7.2.10 Table of Results

Here are briefly shown net fuel reduction results for each vehicle type, based on the simulations done in this study. Different engine sizes are not differentiated, because the effect of drive cycle and control logic are so remarkable. Basically, these results demonstrate that, even with rather simple control design, benefits can be expected from the E-axle in terms of energy usage and even better results can be expected with optimized system. In overall, each vehicle can achieve fuel savings in loaded drive cycle with full

battery, and correspondingly each vehicle will see increase in consumption when charging empty battery by driving. The balance between the two is up to optimization, to achieve desired level of net reduction.

Table 2. Net effect results based on the simulations.

	Long-haul truck	Timber truck	Tipper truck
Net savings fuel in - %	1–4	1–9	-1–5

7.2.11 Discussion of Real Vehicle vs Simulated Vehicle

As it was noticed along the results shown before, the simulated vehicle couldn't always exactly match that of the logged actual vehicle in terms of energy usage. The further the simulated vehicle is from the actual vehicle, the less inaccurate and useful the results will be. During these simulations, it was noticed that matching of the elevation profile was the most crucial for how well the simulated vehicle could match energy usage of the actual vehicle. It is also well known that elevation changes affect movement of loaded truck heavily. There is also margin of error in the engine torque graphs, fuel maps, drivetrain, transmission control, chosen E-axle components, drive cycle etc. which all have their effect on the movement of the vehicle. However, all the used parameters here were believable for trucks and the resisting parameters for the vehicles were also based on quite recent studies and were in the range which is often seen in literature for these sorts of vehicles. Also, the results achieved for the simulated vehicles are believable for trucks as well. These results demonstrate that basically every simulated vehicle here can achieve fuel savings with E-axle, but the amount is highly determined by control logic and drive cycle, and since drive cycle cannot often be chosen in real life, the importance of proper control gets emphasized. The importance of accurate model is most crucial when actual control system is to be designed for the E-axle or any other system. The purpose of this study was not to create very accurate model for control design for example, but rather to provide concept level results of what can be the expected potential of E-axle in timber, long-haul and tipper truck use.

7.2.12 Estimated Auxiliaries Energy

Estimated energy usage on auxiliary devices was calculated for timber truck based on logged data. For long-haul and tipper truck, there was no reliable data available for the estimations. It was estimated that approximately 18–24 kWh of energy is needed for average loading and unloading operation of timber truck. This was calculated with estimated average engine torque ranging from approximately 230 Nm to 410 Nm during crane operations. Hence, in theory with 20 kWh of usable electrical power, it could be possible to do at least half of one unloading/loading operation with electrical energy. This is purely theoretical estimations based on logged data, to give an idea of the energy ranges.

7.3 Summary of Results

These concept level results show that E-axle equipped trailer could provide fuel savings with every tested vehicle type. All in all, similar results were seen between each simulation since the E-axle configuration was the same for each vehicle. Based on these results the amount of savings varies between vehicle types, since they all have different type of typical drive cycles and different vehicle specifications as well. However, let us not forget, that these are concept level study results, where control logic for the E-axle was the same for each vehicle and thus not optimal for any, and the fuel maps for the engine were generated and not from measured data. With good, optimized control logic, better results can be expected. It is difficult to estimate how much the results shown here would change, if simulated with fuel maps from real vehicles since the E-axle control logic also has huge effect on the fuel saving potential. However, these results clearly show that with E-axle, the overall performance of the vehicle will surpass the performance of a vehicle without E-axle. It was also shown that, with E-axle, significant portion of the braking energy could potentially be recuperated. The maximum saved braking energy ranged around 60 %. The overall error of the results is difficult estimate, due to the amount of affecting variables. Net fuel savings considering both the increase caused by regeneration driving and the decrease caused by the E-axle boosting showed possible net reduction with used parameters to be around -1 – 9 %, depending on vehicle and drive cycle, which suggests that E-axle can be feasible solution with proper configuration. The

net savings were highest with timber truck and lowest with tipper truck. It is expected that better net effect results are possible with optimized control and vehicle configuration.

Even if direct comparison of vehicle with downgraded engine and E-axle, and the regular vehicle is not optimal by using logged drive cycles, the results achieved here show that with downgraded engine, practically the same level of performance can be achieved. Simulating different vehicle with a logged drive cycle from another vehicle puts limitations for the overall performance, because instead of driving the E-axle powered vehicle the way that it is best suited for it, the vehicle instead tries to follow the performance of the non-downgraded vehicle as if there is no difference between the vehicles. Also, in the case of regular vehicle with E-axle, the logged drive cycle profile will limit the performance of the E-axle, especially if there are many high hills in the drive cycle, which will then give higher fuel consumption reduction. Such result is not necessarily wrong but also does not necessarily represent real driving very well. In this study, some drive cycles were modified in order to see better pure comparison between different configurations. The vehicles in this study were modeled as 2-axle longitudinal model with lumped mass, which of course adds some limitations. For example, trailer and truck are not one single system in real life but instead two different bodies which also have relative motion happening between them. However, from the longitudinal motion perspective, the difference is negligible.

The shortest driving distances according to data used in this study was with tipper truck, ranging from just couple of kilometers up to about 100 km. Longest driving distances were quite obviously with long-haul truck, which was continuously driving the same route of approximately 340 km per direction. In the middle ground was timber truck, which driving distances were circling around 100 km. With same battery sizes and same amount of battery energy usage, the regeneration power has to be greater for shorter driving distances. With long driving distance, it is possible to use lower charging power and divide the charging time for longer period of time. If driving of a loaded truck with full battery in the beginning is considered, it seems that even with quite small nominal battery size of 20 kWh, it may be possible to gain quite remarkable fuel savings.

REFERENCES

ACS, 2022. ACS News Service Weekly PressPac: June 08, 2022, Lithium-ion batteries that last longer in extreme cold [online document]. Available: https://www.acs.org/pressroom/presspacs/2022/acs-presspac-june-8-2022/lithium-ion-batteries-that-last-longer-in-extreme-cold.html [Accessed 7.7.2023].

Alexander, A., Kelleter, A., Usbeck, S., Knappenberger, U., 2018. Electric machines as drives. In book: Reif, K. (edit.) Automotive Handbook. 10th edition. Karlsruhe, Robert Bosch GmbH, P.844–857. ISBN 978-1-119-53081-7

Argue, C., 2020. What 6,000 EV batteries tell us about EV battery health, State of charge (SOC) and the buffer effect [online document]. Available: https://www.geotab.com/blog/ev-battery-health/ [Accessed 8.7.2023]

Battery University, 2019. BU-1002a: Hybrid Electric Vehicles and the Battery, Hybrid Electric Vehicle (HEV) [online document]. Available: https://batteryuniversity.com/article/bu-1002a-hybrid-electric-vehicles-and-the-battery [Accessed 8.7.2023].

Benz, S., Pankiewitz, C., Fink, H., 2018. Drive batteries. In book: Reif, K. (edit.) Automotive Handbook. 10th edition. Karlsruhe, Robert Bosch GmbH, P. 1322–1329. ISBN 978-1-119-53081-7

Birk, M., Dragon, L., Niethammer, R., Boros, I., Wüst, K., 2018. Motor Vehicle Dynamics. In book: Reif, K. (edit.) Automotive Handbook. 10th edition. Karlsruhe, Robert Bosch GmbH, P. 930–966. ISBN 978-1-119-53081-7

BorgWarner, 2023. Electric Drive Motors, 240 Permanen Magnet Synchronous Drive Motor [online document]. Available: https://www.borgwarner.com/technologies/electric-drive-motors [Accessed 8.7.2023]

Bosch, 2020. Bosch and Weichai Power increase efficiency of Weichai truck diesel engines to 50 percent [online document]. Available: https://www.bosch-presse.de/pressportal/de/en/bosch-and-weichai-power-increase-efficiency-of-weichai-truck-diesel-engines-to-50-percent-218880.html [Accessed 8.7.2023]

Boyrd, 2023. The Importance of Inverter Cooling for Electric Vehicles [online document]. Available: https://www.boydcorp.com/resources/resource-center/blog/importance-of-inverter-cooling-for-electric-vehicles.html [Accessed 8.7.2023].

Carnota M. F., 2020. Investigation of the potential of e-axles for trucks. [online document]. KTH Royal Institute of Technology School of Engineering Sciences. Available: http://kth.diva-portal.org/smash/record.jsf?pid=diva2%3A1503980&dswid=-8449 [Accessed 7.7.2023]. 52 pp.

Chen, D., Jiang, J., Kim, G. H., Yang, C., Pesaran, A., 2015. Comparison of different cooling methods for lithium-ion battery cells. Elsevier. https://doi.org/10.1016/j.applthermaleng.2015.10.015

Dragonfly Energy, 2022. What is Thermal Runaway In Batteries? [online document] Available: https://dragonflyenergy.com/thermal-runaway/ [Accessed 7.7.2023].

EatonVideos, 2020. Inverters in electric vehicles [online document]. Available: https://www.youtube.com/watch?v=Yz_STYgws9I [Accessed 7.3.2023].

E-mobility Engineering, 2023. E-axles [online document]. Available: https://www.emobility-engineering.com/eaxle-transmission/ [Accessed 8.7.2023].

European Commission, 2023. COM(2023) 88 final [online document]. Available from: https://climate.ec.europa.eu/system/files/2023-02/policy_transport_hdv_20230214_proposal_en_0.pdf [Accessed: 10.3.2023]

European Commission, 2023. Reducing CO_2 emissions from heavy-duty vehicles [online document]. Available: https://climate.ec.europa.eu/eu-action/transport-emissions/road-transport-reducing-co2-emissions-vehicles/reducing-co2-emissions-heavy-duty-vehicles_en [Accessed 8.7.2023].

Han, X., Languang, L., Yuejiu, Z., Xuning, F., Zhe, L., Jianqiu, L., Minggao, O., 2019. A review on the key issues of the lithium ion battery degradation among the whole life cycle. Elsevier. https://doi.org/10.1016/j.etran.2019.100005

Heon, M., 2018. Modeling and simulation of a hybrid powertrain. [online document]. KTH Royal Institute of Technology School of Electrical Engineering and Computer Science. Available: http://kth.diva-portal.org/smash/record.jsf?pid=diva2%3A1249494&dswid=5719 [Accessed 7.7.2023]. 88 p.

Huber, T., 2018. Hybrid drives. In book: Reif, K. (edit.) Automotive Handbook. 10th edition. Karlsruhe, Robert Bosch GmbH, P. 822–833. ISBN 978-1-119-53081-7

IEA, 2022. Global EV Outlook 2022, Securing supplies for an electric future [online document]. France: IEA. Available: https://iea.blob.core.windows.net/assets/e0d2081d-487d-4818-8c59-69b638969f9e/GlobalElectricVehicleOutlook2022.pdf [Accessed 8.7.2023]

Jagdale, S., 2023. Understanding the Powertrain of an Electric Vehicle [online document]. Available: https://www.powerelectronicsnews.com/understanding-the-powertrain-of-an-electric-vehicle/ [Accessed 8.7.2023].

Kim, S.H., 2016. Electric Motor Control – DC, AC and BLDC Motors. 1st edition. Elsevier Science, 438 p. ISBN 978-0-12-812138-2

Koch, T., Michler, M., Oelschlegel H., Scharrer, O., 2018. Reciprocating-piston engine. In book: Reif, K. (edit.) Automotive Handbook. 10th edition. Karlsruhe, Robert Bosch GmbH, P. 494–533. ISBN 978-1-119-53081-7

Köller, S., Uerlich, R., Westphal, C. et al. Design of an Electric Drive Axle for a Heavy Truck. ATZ Heavy Duty worldw 14, 20–25 (2021). https://doi.org/10.1007/s41321-021-0420-8

Liikenne ja viestintäministeriö, 2020, Tieliikennelaki. [online document]
Available: https://www.finlex.fi/fi/laki/ajantasa/2018/20180729 [Accessed 7.7.2023]

Long Run, 2023, Design and implantation of an e-axle to the baseline truck [online document]
Available: https://h2020-longrun.eu/design-and-implementation-of-an-e-axle-to-the-baseline-truck/ [Accessed 7.7.2023]

Lundberg, P., 2014. Investigation of the transient nature of rolling resistance on an operating Heavy Duty Vehicle. [online document]. Umeå University, Faculty of Science and Technology, Department of Physics. Available: http://umu.diva-portal.org/smash/record.jsf?pid=diva2%3A747189&dswid=2473 [Accessed 7.7.2023]. 79 p.

Mahajan, J.2020. Understanding Battery Usable Capacity [online document]. Available: https://www.linkedin.com/pulse/understanding-battery-usable-capacity-jaywant-mahajan [Accessed 8.7.2023].

Mäkelä, M., Soininen, L., Tuomola, S., Öistämö, J., 2015. Tekniikan Kaavasto. 15th edition. Porvoo: Bookwell Oy, 205 p. ISBN 978-952-5491-48-7

Mäkipirtti, M., 2011. Sisu – Ajoneuvot Suomessa 4. 2nd edition. Tampere: Apali Oy, 264 p. ISBN 978-952-5877-05-2

MathWorks, 2023a. Battery (System-Level), Generic system level battery [online document]. Available: https://se.mathworks.com/help/sdl/ref/batterysystemlevel.html [Accessed 8.7.2023].

MathWorks, 2023b. Longitudinal Driver, Longitudinal speed-tracking controller [online document]. Available:

https://se.mathworks.com/help/vdynblks/ref/longitudinaldriver.html [Accessed 8.7.2023].

MathWorks, 2023c. Generic Engine, Generic internal combustion engine [online document]. Available: https://se.mathworks.com/help/sdl/ref/genericengine.html [Accessed 8.7.2023].

MathWorks, 2023d. Vehicle Body, Two-axle vehicle with longitudinal dynamics and motion and adjustable mass, geometry, and drag properties [online document]. Available: https://se.mathworks.com/help/sdl/ref/vehiclebody.html [Accessed 8.7.2023].

MathWorks, 2023e. Tire (Friction Parameterized), Tire with friction parameterized in terms of static and kinetic coefficients [online document]. Available: https://se.mathworks.com/help/sdl/ref/tirefrictionparameterized.html [Accessed 8.7.2023].

MathWorks, 2023f. Motor & Drive (System Level), Generic motor and drive with closed-loop torque control [online document]. Available: https://se.mathworks.com/help/sps/ref/motordrivesystemlevel.html [Accessed 8.7.2023].

MathWorks, 2023g. DC-DC Converter, Behavioral model of power converter [online document]. Available: https://se.mathworks.com/help/sps/ref/dcdcconverter.html [Accessed 8.7.2023].

Nieminen, J., 2020. Sähköautojen moottorityypit, Harvinaisilla maametalleilla vai ilman? [online document] Available: https://tekniikanmaailma.fi/lehti/19b-2020/harvinaisilla-maametalleilla-vai-ilman/ [Accessed 7.7.2023]

Omron, 2023. inverters [online document]. Available: https://www.ia.omron.com/support/guide/9/introduction.html [Accessed 7.3.2023].

OSM Energy, 2020. Lithium-ion Battery Energy Density, High energy density batteries. [online document]. Available: https://osmbattery.com/uncategorized/lithium-ion-battery-energy-density/ [Accessed 13.7.2023]

Oswos, 2023. Losses in Electric Motors [online document]. Available: https://oswos.com/motor-losses/ [Accessed 7.3.2023].

Rahkola P., 2019. Raskaan kaluston VECTO-simulointi Suomessa [online document]. Suomi: Liikenne- ja viestintävirasto Traficom. Available: https://www.traficom.fi/sites/default/files/media/publication/Vecto_2018_Traficom_tutkimuksia_13_2019%20(002).pdf [Accessed 1.2.2023].

Ritters, K., Frerichs, L., Heuser, T. et al. Investigation of Electrified Trailer Axles by Use of a Functional Model. ATZ Heavy Duty worldw 12, 60–65 (2019). https://doi.org/10.1007/s41321-019-0039-1

Scania, 2021. 2021: The new Scania Super powers profitability [online document]. Available: https://www.scania.com/group/en/home/about-scania/heritage/corporate-milestones/2021-the-new-scania-super-powers-profitability.html [Accessed 8.7.2023]

Šimić, Zvonimir & Topić, Danijel & Knežević, Goran & Pelin, Denis. (2021). Battery energy storage technologies overview. *International journal of electrical and computer engineering systems*. Vol. 12. 53-65. https://doi.org/10.32985/ijeces.12.1.6.

Thakur, D., 2021. Electric Vehicle Architecture & EV Powertrain Components [online document]. Available: https://e-vehicleinfo.com/electric-vehicle-architecture-ev-powertrain-components/ [Accessed 8.7.2023].

The American Society of Mechanical Engineering, 2023. Advancing Battery Technology for Modern Innovations [online document]. Available: https://www.asme.org/topics-resources/content/advancing-battery-technology-for-modern-innovations [Accessed 5.7.2023]

Tremblay, O., Dessaint, L. A., Dekkiche, A. I., (2007). A Generic Battery Model for the Dynamic Simulation of Hybrid Electric Vehicles. VPPC 2007 - Proceedings of the 2007 IEEE Vehicle Power and Propulsion Conference. 284 - 289. 10.1109/VPPC.2007.4544139.

TÜV SÜD, 2023, Aut omotive Functional Safety According to ISO 26262, What is ISO 26262? [online document] Available: https://www.tuvsud.com/en/industries/mobility-and-automotive/automotive-and-oem/iso-26262-functional-safety [Accessed 7.7.2023]

TÜV SÜD, 2023, UN ECE R100 Standard Regulation, ECE R100 REV Overview. [online document] Available: https://www.tuvsud.com/en/e-ssentials-newsletter/past-topics/what-revision-2-of-ece-r100-means-for-rechargeable-battery-manufacturers [Accessed 7.7.2023]

University of Washington, 2023. Lithium-ion Battery, What are some advantages of Li-ion batteries? [online document]. Available: https://www.cei.washington.edu/education/science-of-solar/battery-technology/ [Accessed 13.7.2023]

Wafzig, J., 2018. Drivetrain with hybrid drives. In book: Reif, K. (edit.) Automotive Handbook. 10th edition. Karlsruhe, Robert Bosch GmbH, P. 812–816. ISBN 978-1-119-53081-7

Wipke, Keith & Cuddy, Matthew & Burch, Steven. (1999). ADVISOR 2.1: A User-Friendly Advanced Powertrain Simulation using a Combined Backward/Forward Approach. Vehicular Technology, IEEE Transactions on. 48. 1751 - 1761. 10.1109/25.806767.

Wong, J. Y, 2008. Theory of Ground Vehicles. 4th edition. Wiley, 592 p. ISBN 978-0470170380

X-Engineering, 2023, EV design – battery calculation. [online document] Available: https://x-engineer.org/ev-design-battery-calculation/ [Accessed 7.7.2023]

Xue, Q., Zhang, X., Teng, T., Zhang, J., Feng, Z., Lv, Q., 2020. A Comprehensive Review on Classification, Energy Management Strategy, and Control Algorithm for Hybrid Electric Vehicles. Energies 13, 5355. https://doi.org/10.3390/en13205355